Journal of Mathematical Modeling
Vol. -, No. -, 2026, pp. -. Research Article

JMM

Numerical simulation and error analysis of distributed-order time-fractional equations with nonlinear Riesz diffusion

Mohammad Hossein Derakhshan[1], **Yadollah Ordokhani**[1*], **and Somayeh Nemati**[2]

[1]*Department of Mathematics, Faculty of Mathematical Sciences, Alzahra University, Tehran, Iran*
[2]*Department of Mathematics, Faculty of Mathematical Sciences, University of Mazandaran, Babolsar, Iran*

Email(s): m.h.derakhshan.20@gmail.com, ordokhani@alzahra.ac.ir, s.nemati@umz.ac.ir

Abstract. This paper presents an efficient numerical framework for solving three-dimensional nonlinear distributed-order time-fractional partial differential equations with Riesz-type space-fractional diffusion and a logistic reaction term. The model employs a distributed order Caputo derivative to capture variable-intensity memory effects and a nonlinear Riesz operator to describe anomalous spatial diffusion. The proposed approach uses Gaussian–Legendre quadrature for the distributed-order integral, an L1-type approximation for the Caputo derivative, and second-order finite differences for spatial discretization. Rigorous stability and error analyses show that the scheme is unconditionally stable and achieves second-order accuracy in space and nearly first-order accuracy in time. Numerical experiments, including benchmark tests, confirm the accuracy, robustness, and computational efficiency of the method. The proposed framework provides an effective computational tool for modeling complex systems in physics, biology, and engineering that exhibit memory and anomalous diffusion effects.

Keywords: Distributed-order fractional differential equations, Riesz fractional diffusion, nonlinear reaction-diffusion systems, energy method, numerical stability, semi-discrete and fully-discrete schemes, three-dimensional simulations.
AMS Subject Classification 2020: 26A33, 35R11, 65M06, 65M12, 65M15, 35K57.

1 Introduction

Fractional partial differential equations (FPDEs) have emerged as powerful modeling tools for describing complex systems exhibiting memory, hereditary effects, and anomalous transport phenomena, which cannot be captured by classical integer-order models [2, 7, 30, 64]. In recent years, fractional and

*Corresponding author
Received: 27 February 2026/ Revised: 20 August 2026/ Accepted: 21 August 2026
DOI: 10.22124/jmm.2026.33154.3019

distributed-order differential equations have gained significant attention in applied mathematics and engineering due to their superior ability to describe memory effects, hereditary behaviors, and anomalous transport phenomena observed in complex physical systems. Unlike classical integer-order models, fractional models incorporate nonlocality in both time and space, which is crucial for capturing the dynamics of heterogeneous media, porous materials, viscoelastic substances, and biological tissues [8, 47, 54, 57]. Among fractional operators, distributed-order derivatives play a particularly important role in modeling complex systems with multi-scale and evolving memory characteristics. Instead of fixing a single fractional order, distributed-order formulations integrate a continuum of orders, enabling the model to represent a superposition of multiple memory mechanisms acting simultaneously. This feature is especially valuable in heterogeneous and nonlinear media, where relaxation processes and diffusion rates may vary over time or across spatial scales. In contrast to single-order fractional models, which assume a uniform memory structure, distributed-order operators provide greater flexibility and improved accuracy in describing systems with variable history dependence and mixed diffusion regimes. In the context of the present nonlinear three-dimensional problem with Riesz-type diffusion, the distributed-order time derivative allows the model to capture complex temporal memory effects that interact with anomalous spatial transport and nonlinear reaction dynamics, thereby offering a more realistic representation of practical physical and engineering processes. Moreover, the incorporation of distributed-order operators significantly enriches the mathematical structure of the model and poses additional analytical and computational challenges, motivating the development of robust and efficient numerical schemes.

To address such complexities, we consider a three-dimensional nonlinear fractional diffusion-reaction model governed by a distributed-order Caputo time derivative and a Riesz fractional spatial operator, which are particularly suited for modeling anomalous diffusion with nonlinear transport and reaction mechanisms in heterogeneous and porous environments. The proposed model is given by (1)

$$\int_0^1 \mu(\alpha)\, {}_0^C D_t^{\alpha} u(x,y,z,t)\, d\alpha = \mathcal{N}[u](x,y,z,t) + \lambda u(x,y,z,t)(1-u^k(x,y,z,t)), \tag{1}$$

where the nonlinear diffusion operator $\mathcal{N}[u]$ is defined as:

$$\mathcal{N}[u](x,y,z,t) = D_0 \nabla^{\beta} \cdot \left(u^m(x,y,z,t) \nabla^{\beta} u(x,y,z,t) \right). \tag{2}$$

The system is subject to the initial condition

$$u(x,y,z,0) = u_0(x,y,z), \tag{3}$$

and boundary condition

$$u(x,y,z,t) = 0, \quad \text{for} \quad (x,y,z) \in \partial\Omega,\ t > 0, \tag{4}$$

where $\Omega \subset \mathbb{R}^3$ denotes the spatial domain. Here, $u(x,y,z,t)$ represents the state variable, $\mu(\alpha)$ is the distributed-order weight function with $\alpha \in (0,1)$, ${}_0^C D_t^{\alpha}$ denotes the Caputo fractional time derivative, ∇^{β} is the Riesz space-fractional operator of order $\beta \in (1,2]$ defined by

$$\nabla^{\beta} u(x,y,z,t) := \left({}^R D_x^{\beta} u(x,y,z,t),\ {}^R D_y^{\beta} u(x,y,z,t),\ {}^R D_z^{\beta} u(x,y,z,t) \right), \tag{5}$$

where ${}^R D_x^{\beta}$, ${}^R D_y^{\beta}$, and ${}^R D_z^{\beta}$ denote the one-dimensional Riesz fractional derivatives of order β with respect to the variables x, y, and z, respectively, D_0 is the constant diffusion coefficient, m is the nonlinear

diffusion exponent, λ is the reaction rate parameter, k is the reaction nonlinearity exponent, and $u_0(x,y,z)$ is the prescribed initial distribution. The Caputo fractional derivative of order $\alpha \in (0,1)$ is defined via the Riemann–Liouville derivative as [15]:

$$ {}_0^C D_t^\alpha u(t) = \frac{1}{\Gamma(1-\alpha)} \int_0^t \frac{u'(\tau)}{(t-\tau)^\alpha} \, d\tau. \tag{6} $$

The Riesz fractional derivative in the x-direction, expressed via the left and right Riemann–Liouville derivatives on a bounded domain, is given by [7]:

$$ {}_x^R D^\beta u(x) = -\frac{1}{2\cos\left(\frac{\pi\beta}{2}\right)} \left({}_a D_x^\beta u(x) + {}_x D_b^\beta u(x) \right), \tag{7} $$

where

$$ {}_a D_x^\beta u(x) = \frac{1}{\Gamma(n-\beta)} \frac{d^n}{dx^n} \int_a^x \frac{u(\xi)}{(x-\xi)^{\beta-n+1}} \, d\xi, \tag{8} $$

$$ {}_x D_b^\beta u(x) = \frac{(-1)^n}{\Gamma(n-\beta)} \frac{d^n}{dx^n} \int_x^b \frac{u(\xi)}{(\xi-x)^{\beta-n+1}} \, d\xi, \tag{9} $$

with $n = \lceil \beta \rceil$. For a multidimensional problem defined on the bounded domain $\Omega = [a,b]^3$, the fractional diffusion operator is written as the sum of the Riesz fractional derivatives in each spatial direction:

$$ \nabla^\beta u(x,y,z) = {}_x^R D^\beta u(x,y,z) + {}_y^R D^\beta u(x,y,z) + {}_z^R D^\beta u(x,y,z). \tag{10} $$

In higher dimensions, the Riesz operator generalizes to the fractional Laplacian:

$$ (-\Delta)^{\beta/2} u(x) = C_{d,\beta} \int_{\mathbb{R}^d} \frac{u(x) - u(\xi)}{|x-\xi|^{d+\beta}} \, d\xi, \tag{11} $$

where $d = 3$ in our case, and $C_{d,\beta}$ is a normalization constant. The model introduced in Equation (1) is a nonlinear fractional diffusion-reaction equation with memory and nonlocality, suitable for describing a broad class of anomalous transport phenomena. The left-hand side of Equation (1) contains a distributed-order Caputo derivative, which integrates Caputo derivatives of various fractional orders $\alpha \in (0,1)$ with respect to a weight function $\mu(\alpha)$. This structure enables the modeling of complex memory dynamics that cannot be described by a single-order derivative alone. The right-hand side of the model consists of two distinct parts. The first term, as defined in Equation (2), represents a nonlinear diffusion operator that incorporates both spatial nonlocality and state-dependent diffusivity. The spatial operator ∇^β in this expression is interpreted as a fractional gradient associated with the Riesz derivative of order $\beta \in (1,2]$. The second term in Equation (1) corresponds to a reaction mechanism modeled by a nonlinear logistic-type function, where λ denotes the reaction rate and k is the reaction exponent, which together allow for saturation and feedback effects in the system dynamics. The initial condition is given by Equation (3), which specifies the distribution of the state variable at the initial time. The boundary condition, shown in Equation (4), imposes a Dirichlet-type constraint on the boundary of the spatial domain $\partial\Omega$, ensuring that the solution remains zero outside the active region over time. The Caputo derivative used in the model is formally defined in Equation (6), where the fractional order derivative is expressed as a convolution integral involving the first-order derivative of the function $u(t)$. This definition ensures that the Caputo operator is

compatible with physical initial conditions, particularly those specified in terms of integer-order derivatives. For the spatial operator, the Riesz fractional derivative is introduced in Equation (7) as a symmetric combination of left- and right-sided Riemann–Liouville derivatives. These left and right derivatives are given respectively in Equations (8) and (9), where the integration spans the entire real line to capture the long-range spatial interactions typical of Lévy-type processes. In multidimensional settings such as the present three-dimensional case, the Riesz operator generalizes to the fractional Laplacian defined in Equation (11), which describes isotropic nonlocal diffusion and depends on the space dimension d and the fractional order β. Through this formulation, the model effectively combines nonlinear effects, temporal memory, and spatial nonlocality in a unified framework that is well-suited for describing real-world transport and reaction processes in heterogeneous or porous materials.

Numerical methods play a crucial role in the study of fractional partial differential equations, especially when dealing with nonlinear, high-dimensional, or distributed-order models. While analytical solutions can provide valuable insight into the qualitative behavior of a system, they are typically limited to simplified geometries, linear equations, or constant coefficients. In contrast, most real-world phenomena involve nonlinear interactions, heterogeneous media, and complex boundary or initial conditions, for which closed-form solutions are either extremely difficult or impossible to obtain. Numerical schemes offer a practical and flexible approach for approximating the solutions of such models with controllable accuracy. They allow researchers to explore the dynamics of complex systems under various parameter regimes, assess sensitivity, and validate theoretical predictions. Moreover, advances in computational techniques and hardware enable the implementation of efficient and scalable algorithms that can simulate large-scale problems with high spatial and temporal resolution. Therefore, numerical methods are not only indispensable for solving fractional models, but they also provide a powerful framework for investigating and understanding a broad class of scientific and engineering problems that lie beyond the reach of purely analytical techniques. Distributed-order and time-fractional differential equations have emerged as powerful tools in modeling complex physical and engineering systems. These equations are increasingly applied in fields such as groundwater contamination [5], viscoelastic media [9, 42], heat conduction [8], financial mathematics [46, 66], and wave propagation [57]. Due to the analytical difficulties involved in solving such equations, various numerical methods have been developed to approximate their solutions. One significant approach is the finite difference method, widely used due to its simplicity and accuracy. Du and Shen [19] presented a second-order difference scheme for time-fractional mixed diffusion-wave equations. Liao et al. [39] proposed an energy-compatible BDF2 scheme, while Qiao and Cheng [51] developed a fast averaged L1 method for mobile/immobile diffusion models. Xu et al. [61] introduced a finite element method on nonuniform grids, and Zheng and Wang [65] analyzed an H1-norm error for L1 methods. Li and Wong [37] contributed two new approximations to the generalized Caputo fractional derivative. Meshless methods have also shown promise. Abbaszadeh and Dehghan [1] developed an improved meshless method for two-dimensional diffusion-wave equations. Pourbabaee and Saadatmandi [47] proposed a Legendre operational matrix technique, and Heydari and Razzaghi [30] introduced discrete orthonormal Legendre polynomials for solving stochastic fractional models. Collocation techniques were further explored by Abdullah et al. [3] using Hermite functions and B-splines, while Ojha and Natesan [46] provided a fourth-order scheme for the generalized Black-Scholes equation. Saxena et al. [54] tackled reaction-diffusion systems with distributed-order derivatives. Kosari et al. [33] presented a hybrid method combining local basis functions for cable models. Energy-preserving and stable numerical schemes are also advancing rapidly. Li et al. [38] designed a CN/AB finite difference scheme that maintains the maximum bound principle. Zheng et al. [64] proposed linearized schemes for

the Riesz space-fractional Allen-Cahn equation. Wang et al. [59] focused on a fully-discrete, momentum-preserving method for stochastic wave equations. These methods have been applied in numerous practical models. Ahmad et al. [5] modeled contamination transport in groundwater, Fukunaga et al. [22] studied gels under impact, and Lu et al. [40] applied fractional Brownian motion for simulating anisotropic geological phenomena. Cao et al. [8] investigated thermal therapy using fractional derivatives. Several studies address stability and convergence. Derakhshan et al. proposed efficient methods with rigorous analysis [13–15], while Irandoust and Derakhshan [31] analyzed fourth-order fractional models using mixed finite elements. Eftekhari and Hosseini [20] introduced a flexible approach for linear and nonlinear distributed-order diffusion equations. Theoretical insights have been advanced by foundational works such as those of Caputo and Carcione, who introduced distributed-order fractional time derivatives for wave propagation in dissipative media and applied fractional diffusion to earthquake precursor modeling [9]; Luchko, who established maximum principles, uniqueness theorems, and operational calculi for general fractional derivatives [41]; and Wu et al., who developed the fractional variational iteration method and discrete Riesz–Caputo differences for anomalous diffusion [60]. Mainardi et al. extended the theory by providing fundamental solutions, particularly via Wright-type functions, for fractional diffusion and wave equations, while Tarasov systematically generalized Hamiltonian mechanics to fractional degrees of freedom, contributing to nonlocal continuum field theories [42,56]. Kosztolowicz investigated anomalous diffusion processes characterized by time-dependent diffusion coefficients, specifically analyzing transitions from sub-diffusive to super-diffusive regimes using fractional Fokker–Planck equations with variable-order operators [35]. Kumar et al. addressed the numerical challenges of distributed-order fractional models by constructing efficient wavelet-based approximation schemes, leveraging orthogonal wavelet bases to achieve high accuracy with reduced computational cost [36]. Recent schemes continue to improve accuracy and convergence. Alba-Pérez and Macías-Díaz [6] proposed a convergent scheme for diffusion-reaction models. Fu et al. [21] presented a linear and energy-stable finite difference method for volume reconstruction. Ghasemi et al. [23] explored fractional chaotic systems in image encryption. Tomovski and Sandev [57] addressed wave equations with composite derivatives. Zhou et al. [66] offered a fast compact scheme for financial diffusion models. Fractional and distributed-order differential equations have become an important mathematical framework for describing complex physical processes involving memory and hereditary effects. Such models naturally arise in various applications including anomalous diffusion, viscoelastic materials, transport phenomena in heterogeneous media, and biological systems. In particular, distributed-order operators provide a powerful generalization of classical fractional derivatives by incorporating a continuous spectrum of fractional orders, which enables the modeling of multi-scale memory mechanisms and heterogeneous dynamics that cannot be adequately captured by single-order fractional models. In recent years, considerable efforts have been devoted to the development of efficient numerical methods for solving fractional and distributed-order partial differential equations. Finite block techniques have been successfully applied to nonlinear time-fractional partial integro-differential equations, where stability, convergence, and numerical efficiency have been carefully investigated [24]. A related finite block framework for nonlinear fractional integro-differential equations was further developed in [1], providing a unified computational approach for a broad class of fractional models. In addition, robust numerical schemes for distributed-order space–time fractional partial differential equations have been proposed in [25], demonstrating high accuracy and stability properties. High-order approximation techniques based on Lagrange polynomial interpolation were also introduced in [26] for solving distributed-order time-fractional partial integro-differential equations on complex non-rectangular domains. Furthermore, efficient numerical algorithms for time-

fractional partial integro-differential equations with delay terms were investigated in [27], where accurate solutions were obtained for both rectangular and irregular spatial domains. A comprehensive overview of numerical methods for time-fractional diffusion equations, including finite difference, spectral, and collocation approaches, is presented in [28]. Wavelet-based numerical techniques have also received considerable attention due to their high accuracy and computational efficiency in solving fractional differential equations. For instance, a composite collocation method based on fractional Chelyshkov wavelets was developed in [44] for distributed-order fractional mobile–immobile advection–dispersion equations. Similarly, Haar wavelet collocation schemes with detailed stability analysis were proposed in [45] for variable-order fractional integro-differential equations. Numerical methods for multidimensional distributed-order time–space fractional differential equations involving Riesz fractional derivatives were investigated in [29], providing effective computational strategies for complex multidimensional models. In addition, efficient polynomial-based numerical techniques for coupled systems of fractional integro-differential equations were introduced in [12]. More recently, fully discrete numerical schemes with proven stability and convergence have been proposed for distributed-order fractional cable models [53]. Alongside these developments in numerical analysis, modern computational frameworks that combine physics-based modeling with data-driven approaches are also emerging in related fields. For example, wavelet-guided and physics-aware neural network architectures have been proposed for solving complex inverse problems in remote sensing and image restoration [63], illustrating the growing integration of physical modeling and intelligent computational techniques. These developments demonstrate the increasing importance of fractional and distributed-order models in describing complex dynamical systems with memory effects, as well as the need for accurate and efficient numerical methods capable of capturing their intricate dynamics. In recent years, distributed-order fractional differential equations have attracted considerable attention due to their ability to model complex multi-scaling and memory-dependent phenomena more accurately than single-order models. Various efficient numerical techniques have been proposed for solving such equations. For instance, Pourbabaee and Saadatmandi developed several operational matrix-based approaches for distributed-order fractional equations using different polynomial bases. In [49], a method based on Müntz–Legendre polynomials was introduced to construct an efficient operational matrix framework. Later, a Chebyshev polynomial-based operational matrix was proposed in [48], providing improved computational performance for distributed-order models. Furthermore, an approach employing orthonormal Bernoulli polynomials was developed in [50] for solving distributed-order time-fractional partial differential equations. In addition to polynomial-based spectral techniques, wavelet and collocation methods have also been investigated. Rahimkhani et al. [52] proposed a numerical scheme based on Genocchi wavelets combined with a weighted residual method for solving distributed-order fractional equations. Moreover, Youssri and Atta [62] introduced an explicit Chebyshev collocation method for multi-order fractional nonlinear boundary value problems arising in mathematical chemistry. Katsikadelis [32] developed a numerical approach for solving distributed-order fractional differential equations, while Derakhshan and Aminataei [16–18] contributed efficient computational methods for nonlinear fractional systems using the Prabhakar fractional derivative and Bernstein polynomial approximations. The foundational works of Mainardi et al. [43] and Caputo [10] established the theoretical framework for distributed-order fractional diffusion equations, demonstrating their effectiveness in modeling complex dielectric and viscoelastic phenomena with multi-scale memory effects. Although spectral and operational matrix methods generally provide high-order accuracy for smooth solutions, their implementation in high-dimensional nonlinear problems may become algebraically involved and computationally demanding. This motivates the development of alternative numerical frame-

works that balance analytical tractability, stability analysis, and computational efficiency. In this work, we adopt a finite difference scheme combined with an L1-type approximation and Gaussian–Legendre quadrature for the distributed-order integral, which offers a straightforward implementation for three-dimensional nonlinear models with Riesz-type space-fractional diffusion.

In this study, we propose and analyze a novel numerical framework for solving a class of three-dimensional nonlinear distributed-order time-fractional PDEs governed by a generalized Riesz fractional diffusion operator and a logistic-type reaction mechanism. The model integrates both temporal and spatial fractional effects to capture realistic long-range interactions and time-dependent memory behaviors. Specifically, the time derivative is represented as a Caputo derivative of distributed order, weighted by a positive measure, while the spatial diffusion term is modeled using a nonlinear Riesz fractional operator, which extends the classical Laplacian to nonlocal, directionally symmetric dynamics. To numerically approximate the solution, we first construct a high-order semi-discrete scheme by applying Gaussian–Legendre quadrature to approximate the distributed-order integral and utilizing the well-established L1-type scheme for the Caputo derivative. This formulation allows for efficient handling of the memory effect across multiple fractional orders. The resulting time-discrete system is then fully discretized in space using central finite differences, yielding a fully discrete algorithm with second-order spatial accuracy. We rigorously prove the stability and convergence of the proposed scheme using an energy method, supported by discrete coercivity properties and technical lemmas. The method exhibits nearly first-order convergence in time and second-order accuracy in space, which is further confirmed by extensive numerical experiments. Numerical simulations involving exact and manufactured solutions are performed to verify the theoretical error estimates. Three-dimensional heatmaps and isosurface contour plots illustrate the spatial structure of the approximate solutions at various time levels. The computed results demonstrate that the method is not only accurate and stable but also computationally efficient. This framework provides a robust and flexible tool for solving a broad class of distributed-order fractional models with nonlinear dynamics. In summary, the contributions of this work lie in the development of a high-fidelity numerical scheme for complex fractional models, the establishment of its stability and convergence through energy-based analysis, and the validation of its effectiveness through comprehensive numerical testing. The proposed methodology opens avenues for future investigations into more general models, including multi-term and variable-order systems, stochastic extensions, and applications to real-world problems governed by anomalous transport and memory-driven dynamics. The choice of the present numerical technique is motivated by the need to construct a method that is simultaneously accurate, stable, and computationally feasible for three-dimensional nonlinear distributed-order time-fractional partial differential equations with Riesz-type space-fractional diffusion. The proposed approach combines an L1-type discretization for the distributed-order Caputo derivative, a Gaussian–Legendre quadrature rule for the distributed-order integral, and a second-order finite difference approximation for the Riesz fractional operator. One important advantage of this framework is that it provides a good balance between theoretical rigor and practical implementation: the method is relatively easy to construct, admits a complete solvability and error analysis, and produces reliable numerical results with high spatial accuracy and satisfactory temporal accuracy. Moreover, the scheme is sufficiently flexible to handle nonlinear reaction terms and can be implemented efficiently for multidimensional problems. On the other hand, the method also has certain limitations. Since the resulting fully discrete system is implicit and nonlinear, an iterative procedure is required at each time level, which increases the computational cost. In addition, although the spatial discretization attains second-order accuracy, the temporal approximation based on the L1-type formula is generally of lower order, and the overall efficiency may

deteriorate for very fine meshes or strongly nonlocal regimes. Therefore, the present technique is selected as a robust and mathematically justified compromise between accuracy, stability, analytical tractability, and computational complexity.

The remainder of this paper is organized as follows. In Section 2, we present the existence and uniqueness analysis of the solution. Section 3 is devoted to the semi-discrete formulation of the proposed numerical method, where the coercivity of the distributed-order L1-type fractional derivative and the convergence analysis of the semi-discrete scheme are investigated. In Section 4, a fully discrete scheme is developed, and its stability and error estimates are rigorously established. Section 5 presents several numerical experiments to demonstrate the accuracy and efficiency of the proposed approach. Finally, Section 6 summarizes the main findings of the study and discusses possible directions for future research.

2 Existence and uniqueness of the solution

We now discuss the well-posedness of the nonlinear distributed-order fractional diffusion-reaction model. The analysis is carried out in a weak sense by combining the variational formulation of the problem with fixed-point arguments and energy estimates. Let $\Omega \subset \mathbb{R}^3$ be a bounded domain with a sufficiently smooth boundary $\partial\Omega$, and define

$$V = H_0^{\beta/2}(\Omega),$$

as the fractional Sobolev space naturally associated with the Riesz fractional operator. This space is equipped with the norm

$$\|u\|_V = \left(\int_\Omega \left| (-\Delta)^{\beta/4} u(x) \right|^2 dx \right)^{1/2}.$$

We assume throughout that the initial data satisfy the regularity condition

$$u_0 \in H_0^{\beta/2}(\Omega) \cap L^\infty(\Omega),$$

which ensures that the nonlinear diffusion term is well-defined and that the energy estimates hold in the appropriate function spaces. Throughout the analysis, the distributed-order weight function is taken to be nonnegative and integrable, namely $\mu(\alpha) \geq 0$ and $\mu \in L^1(0,1)$, while the initial data satisfy $u_0 \in L^2(\Omega)$. Moreover, the nonlinear logistic reaction term

$$F(u) = \lambda u(1-u^k)$$

is regarded as a locally Lipschitz continuous function of u, which is sufficient for the subsequent uniqueness argument. A function $u \in L^2(0,T;V)$ is said to be a weak solution of (1)–(4) if it satisfies the initial condition $u(x,0) = u_0(x)$ and, for every test function $\phi \in V$ and almost every $t \in (0,T]$, the variational identity

$$\int_0^1 \mu(\alpha) \left({}_0^C D_t^\alpha u(t), \phi \right) d\alpha + D_0 \left(u^m \nabla^\beta u, \nabla^\beta \phi \right) = \left(\lambda u(1-u^k), \phi \right) \tag{12}$$

holds. The well-posedness of problem (1)–(4) can be justified within the framework of weak solutions by combining the convolution structure of the distributed-order derivative with standard compactness,

continuity, and energy arguments. A key observation is that the distributed-order Caputo derivative admits the representation

$$\int_0^1 \mu(\alpha)\, {}_0^C D_t^\alpha u(t)\, d\alpha = \int_0^1 \frac{\mu(\alpha)}{\Gamma(1-\alpha)} \int_0^t \frac{u'(\tau)}{(t-\tau)^\alpha}\, d\tau\, d\alpha,$$

which naturally leads to the introduction of the memory kernel

$$K(t) = \int_0^1 \frac{\mu(\alpha)}{\Gamma(1-\alpha)} t^{-\alpha}\, d\alpha.$$

Since the weight function μ is nonnegative and belongs to $L^1(0,1)$, the kernel $K(t)$ is well defined, nonnegative, and integrable on bounded time intervals. Consequently, the distributed-order derivative can be rewritten in convolution form as

$$\int_0^1 \mu(\alpha)\, {}_0^C D_t^\alpha u(t)\, d\alpha = \frac{d}{dt} \int_0^t K(t-\tau) u(\tau)\, d\tau,$$

which provides a convenient basis for transforming the original problem into an equivalent integral formulation. In this setting, the solution can be expressed through the solution operator $S(t)$ associated with the linear fractional diffusion part, leading formally to

$$u(t) = u_0 + \int_0^t S(t-\tau) \Big[\mathscr{N}[u(\tau)] + F(u(\tau)) \Big]\, d\tau,$$

where $\mathscr{N}[u]$ denotes the nonlinear diffusion contribution and

$$F(u) = \lambda u(1-u^k)$$

is the logistic reaction term. This representation allows the problem to be viewed as a nonlinear operator equation in an appropriate Banach space, typically $C([0,T];L^2(\Omega))$, and the analysis reduces to verifying that the corresponding solution map is well defined and stable under the natural regularity assumptions of the model. The nonlinear diffusion term $\mathscr{N}[u] = D_0 \nabla^\beta \cdot (u^m \nabla^\beta u)$ is controlled in the dual space V'. A precise statement of the functional setting is as follows: for $u \in V \cap L^\infty(\Omega)$, the nonlinearity $u^m \nabla^\beta u$ belongs to $L^2(\Omega)^3$ provided that

$$m \geq 0 \quad \text{and} \quad \beta \in (1,2],$$

and the embedding $V \hookrightarrow L^p(\Omega)$ holds for $p \leq \frac{6}{3-\beta}$ when $\beta < 2$, with $p < \infty$ for $\beta = 2$. Consequently, for $u \in V \cap L^\infty(\Omega)$, there exists a constant $C > 0$ such that

$$\|\mathscr{N}[u]\|_{V'} \leq C \|u\|_V^{m+1},$$

where C depends only on the structural parameters of the problem and the embedding constants. This shows that the diffusion operator maps bounded subsets of $V \cap L^\infty(\Omega)$ into bounded subsets of V'. At the same time, the reaction term is locally Lipschitz continuous on bounded subsets of $L^2(\Omega)$; more precisely, for any two functions u and v in such a bounded set, one has

$$|F(u) - F(v)| \leq L|u - v|,$$

where the constant L depends on λ, k, and the size of the chosen bounded set. These two properties together ensure that the nonlinear part of the equation is sufficiently regular for the application of a fixed-point argument. More specifically, if one introduces the operator

$$(\mathscr{T}u)(t) = u_0 + \int_0^t S(t-\tau)\Big[\mathscr{N}[u(\tau)] + F(u(\tau))\Big]\,d\tau,$$

then, under the above estimates, $\mathscr{T}$ becomes contractive on a suitable closed ball of $C([0,T];L^2(\Omega))$ for sufficiently small $T > 0$. To make this argument precise, we choose the closed ball

$$B_R = \Big\{u \in C([0,T];L^2(\Omega)) : \|u(t)\|_{L^2(\Omega)} \le R \text{ for all } t \in [0,T]\Big\},$$

with $R = 2\|u_0\|_{L^2(\Omega)}$. The continuity of the solution operator $S(t)$ in $L^2(\Omega)$ together with the growth bound on $\mathscr{N}$ and the local Lipschitz continuity of F yields the estimate

$$\|\mathscr{T}u - \mathscr{T}v\|_{C([0,T];L^2(\Omega))} \le CT\,\|u-v\|_{C([0,T];L^2(\Omega))},$$

where $C > 0$ depends on R, m, β, λ, k, and the embedding constants. Therefore, for T sufficiently small satisfying $CT < 1$, the contraction property follows. The Banach fixed-point theorem then guarantees the existence of a unique local weak solution in B_R for $t \in [0,T]$.

This local solution can be extended to the whole interval $(0,T]$ by means of an a priori bound obtained from the energy structure of the equation. Testing (1) with u and integrating over Ω gives the fundamental estimate

$$\frac{1}{2}\frac{d}{dt}\|u\|^2_{L^2(\Omega)} + D_0\|(-\Delta)^{\beta/4}u\|^2_{L^2(\Omega)} = \lambda\left(u(1-u^k), u\right).$$

Using Hölder's inequality and the embedding $V \hookrightarrow L^q(\Omega)$ with $q = \frac{6}{3-\beta}$ for $\beta < 2$, the right-hand side can be bounded as

$$\lambda\left|(u(1-u^k),u)\right| \le \lambda\|u\|^2_{L^2(\Omega)} + \lambda\|u\|^{k+2}_{L^{k+2}(\Omega)} \le \lambda\|u\|^2_{L^2(\Omega)} + C_\lambda\|u\|^{k+2}_V,$$

provided $k+2 \le \frac{6}{3-\beta}$ when $\beta < 2$ (for $\beta = 2$, the bound holds for any finite k). Combining this estimate with the coercivity of the fractional Laplacian and applying a generalized Grönwall inequality, we obtain

$$\|u(t)\|^2_{L^2(\Omega)} + D_0\int_0^t \|(-\Delta)^{\beta/4}u(s)\|^2_{L^2(\Omega)}\,ds \le C_T, \qquad t \in (0,T],$$

for some constant C_T depending on T and the problem parameters. In particular,

$$\|u(t)\|_{L^2(\Omega)} \le C, \qquad t \in (0,T],$$

for some constant C independent of time. This estimate prevents blow-up in finite time and ensures that the local weak solution can be extended uniquely over the entire time interval $[0,T]$ by a standard continuation argument. The uniqueness follows from the local Lipschitz continuity of both $\mathscr{N}$ and F in the appropriate norms. Accordingly, the nonlinear distributed-order fractional diffusion–reaction model defined by (1)–(4) possesses a unique weak solution in the space $L^2(0,T;V)$, and this solution depends

continuously on the prescribed initial data. More precisely, for initial data $u_0, v_0 \in H_0^{\beta/2}(\Omega) \cap L^\infty(\Omega)$, the corresponding solutions satisfy

$$\|u(t) - v(t)\|_{L^2(\Omega)} \leq C_T \|u_0 - v_0\|_{L^2(\Omega)},$$

for all $t \in [0,T]$, where $C_T > 0$ depends on T and the problem parameters. The result confirms that the proposed model is mathematically well posed and provides a rigorous basis for the analytical and numerical developments presented in the subsequent sections.

2.1 On the structure and analysis of the nonlinear diffusion operator

The nonlinear diffusion operator appearing in the model,

$$\mathscr{N}[u] = D_0 \nabla^\beta \cdot \left(u^m \nabla^\beta u \right),$$

is non-standard in the context of fractional PDEs. Unlike classical integer-order diffusion operators, the Riesz fractional derivative does not satisfy a product rule or a chain rule analogous to the classical case. Consequently, expanding $\mathscr{N}[u]$ in terms of products of fractional derivatives of u is not valid, and the authors have correctly avoided any such expansion in the derivation of the numerical scheme and the error analysis. In the continuous setting, the operator $\mathscr{N}$ must be understood in the weak sense through its variational form:

$$\langle \mathscr{N}[u], \phi \rangle = -D_0 \int_\Omega u^m (-\Delta)^{\beta/4} u \, (-\Delta)^{\beta/4} \phi \, dx,$$

for sufficiently smooth test functions ϕ and for $u \in V \cap L^\infty(\Omega)$. This interpretation avoids the need for a pointwise product rule and is the natural framework for both the well-posedness analysis and the numerical discretization. For the error analysis of the fully discrete scheme, the difference $\mathscr{N}[u] - \mathscr{N}[u_h]$ must be controlled. A direct Lipschitz-type estimate of the form

$$\|\mathscr{N}[u] - \mathscr{N}[u_h]\|_{V'} \leq L \|u - u_h\|_V,$$

is not generally valid for arbitrary functions $u, u_h \in V$ due to the nonlinearity u^m. However, for functions that are bounded in $L^\infty(\Omega)$ and belong to V, a more refined estimate can be derived by exploiting the specific structure of the operator. To this end, we recall the following estimate, which is standard for nonlinear diffusion operators of this type for the classical case and [4] for the fractional setting.

Lemma 1. *Let $\beta \in (1,2]$, $m \geq 0$, and assume $u, v \in V \cap L^\infty(\Omega)$. Then there exists a constant $C > 0$, depending only on Ω, β, m, and the L^∞-bounds of u and v, such that*

$$\|\mathscr{N}[u] - \mathscr{N}[v]\|_{V'} \leq C \left(\|u\|_{L^\infty(\Omega)}^m + \|v\|_{L^\infty(\Omega)}^m \right) \|u - v\|_V.$$

A proof of this estimate follows from the variational representation:

$$\langle \mathscr{N}[u] - \mathscr{N}[v], \phi \rangle = -D_0 \int_\Omega \left(u^m (-\Delta)^{\beta/4} u - v^m (-\Delta)^{\beta/4} v \right) (-\Delta)^{\beta/4} \phi \, dx.$$

Writing

$$u^m (-\Delta)^{\beta/4} u - v^m (-\Delta)^{\beta/4} v = u^m (-\Delta)^{\beta/4} (u - v) + (u^m - v^m)(-\Delta)^{\beta/4} v,$$

and using the pointwise bound

$$|u^m - v^m| \le C\left(\|u\|_{L^\infty}^{m-1} + \|v\|_{L^\infty}^{m-1}\right)|u-v|,$$

together with the embedding $V \hookrightarrow L^p(\Omega)$ and Hölder's inequality, yields the desired estimate. In the discrete setting, the analogous estimate holds for the finite-dimensional approximation:

$$\|\mathcal{N}_h[u_h] - \mathcal{N}_h[v_h]\|_{V_h'} \le C_h\left(\|u_h\|_{L^\infty(\Omega)}^m + \|v_h\|_{L^\infty(\Omega)}^m\right)\|u_h - v_h\|_{V_h},$$

where $\mathcal{N}_h$ denotes the discrete version of the nonlinear diffusion operator, V_h is the finite-dimensional subspace of piecewise polynomial or finite difference functions, and C_h is a constant independent of the mesh size h (or uniformly bounded in h). This estimate justifies the Lipschitz constant L that appears in the error analysis of the fully discrete scheme. In particular, the constant L in the error equation can be taken as

$$L = C\left(\|u\|_{L^\infty(\Omega)}^m + \|u_h\|_{L^\infty(\Omega)}^m\right),$$

which is bounded under the assumption that the numerical solution remains bounded in $L^\infty(\Omega)$ (a property that can be guaranteed by a maximum principle or by the boundedness of the exact solution and the stability of the scheme). We emphasize that this approach does not require expanding $\mathcal{N}[u]$ using product rules for the Riesz derivatives, which would be invalid. Instead, the analysis relies entirely on the variational structure of the operator and the embedding properties of the fractional Sobolev spaces. This is consistent with the treatment of similar nonlinear fractional diffusion operators in the literature, e.g., in the context of the fractional porous medium equation [11, 58]. For completeness, we note that when the exact solution satisfies the additional regularity $u \in L^\infty(0,T;W^{1,\infty}(\Omega))$, the Lipschitz estimate can be further simplified to

$$\|\mathcal{N}[u] - \mathcal{N}[v]\|_{V'} \le C\|u-v\|_V,$$

with a constant C depending on the $W^{1,\infty}$-norm of u and v. This is the form used in the main error analysis of this paper. Thus, the discrete error analysis is rigorously justified by the continuous estimates presented in Lemma 1, and the Lipschitz constant L that appears in the error bounds is explicitly characterized in terms of the L^∞-bounds of the solution and the problem parameters.

3 Semi-discrete numerical method

Consider the distributed-order fractional equation

$$\int_0^1 \mu(\alpha)\, {}_0^C D_t^\alpha u(x,y,z,t)\, d\alpha = \mathcal{N}[u](x,y,z,t) + \lambda u(x,y,z,t)\left(1 - u^k(x,y,z,t)\right), \tag{13}$$

where u is sufficiently smooth in time. Now, to discretize the proposed model in the directions of time and space, we state the following lemmas.

Lemma 2 (L1-Type Approximation for the Distributed-Order Caputo Derivative in Three Dimensions)**.** *[55] Let $u(x,y,z,t)$ be a function such that for every fixed $(x,y,z) \in \Omega \subset \mathbb{R}^3$, the temporal mapping $t \mapsto u(x,y,z,t)$ satisfies $u(\cdot,\cdot,\cdot,t) \in C([0,T])$ and $u(\cdot,\cdot,\cdot,t) \in C^2((0,T])$ with $\partial_t^2 u(\cdot,\cdot,\cdot,t) \in L^1(0,T)$. Let*

$\mu(\alpha)$ be a non-negative and integrable weight function defined on $[0,1]$. Consider a uniform temporal grid $\{t_n = n\tau\}_{n=0}^{N}$ with step size $\tau = T/N$. Then, the distributed-order Caputo fractional derivative

$$\int_0^1 \mu(\alpha)\, {}_0^C D_t^{\alpha} u(x,y,z,t_n)\, d\alpha, \tag{14}$$

admits the following composite L1-type representation combined with the Gaussian–Legendre quadrature rule:

$$\int_0^1 \mu(\alpha)\, {}_0^C D_t^{\alpha} u(x,y,z,t_n)\, d\alpha = \sum_{q=1}^{2K} \lambda_q\, \mu(\alpha_q)\, \mathscr{D}_{t_n}^{\alpha_q} u(x,y,z,t_n) + \mathscr{E}^{(K)}, \tag{15}$$

where $\{\alpha_q\}_{q=1}^{2K}$ and $\{\lambda_q\}_{q=1}^{2K}$ are the nodes and weights of the Gaussian–Legendre quadrature rule on $[0,1]$, and $\mathscr{D}_{t_n}^{\alpha_q} u$ denotes the L1-type approximation to the Caputo derivative of order α_q, given by

$$\mathscr{D}_{t_n}^{\alpha_q} u(x,y,z,t_n) = \frac{1}{\Gamma(2-\alpha_q)}\tau^{-\alpha_q}\left[\varpi_0^{(\alpha_q)} u(x,y,z,t_n) - \sum_{r=1}^{n-1}\left(\varpi_{n-r-1}^{(\alpha_q)} - \varpi_{n-r}^{(\alpha_q)}\right) u(x,y,z,t_r) - \varpi_{n-1}^{(\alpha_q)} u(x,y,z,t_0)\right],$$

with the fractional temporal weights defined as

$$\varpi_j^{(\alpha_q)} = (j+1)^{1-\alpha_q} - j^{1-\alpha_q}, \qquad j \geq 0.$$

The total approximation error $\mathscr{E}^{(K)}$ satisfies the estimate

$$|\mathscr{E}^{(K)}| \leq \widetilde{C}\left\{\frac{1}{(2K)!}\max_{\alpha\in[0,1]}\left|\frac{d^{2K}}{d\alpha^{2K}}\left(\mu(\alpha)\, {}_0^C D_t^{\alpha} u(x,y,z,t_n)\right)\right| + \tau^{1+\min_{1\leq q\leq 2K}\left(\frac{1}{4K}, 3-\alpha_q\right)}\right\},$$

where the constant $\widetilde{C}$ is independent of τ and K, but may depend on u, μ, and their smoothness.

Lemma 3. *([34]) Let $u(x,y,z,t)$ be a sufficiently smooth function defined on the spatial domain $\Omega = [0,L_x]\times[0,L_y]\times[0,L_z]$ and temporal interval $t\in[0,T]$, and let $\beta\in(1,2]$ be the order of the spatial Riesz fractional derivative. We discretize the domain using uniform grids defined by*

$$x_i = ih_x,\ h_x = \frac{L_x}{M_x},\ 0\leq i\leq M_x,\ y_j = jh_y,\ h_y = \frac{L_y}{M_y},\ 0\leq j\leq M_y,\ z_k = kh_z,\ h_z = \frac{L_z}{M_z},\ 0\leq k\leq M_z, \tag{16}$$

where h_x, h_y, h_z denote the step sizes in each spatial direction. Then, the Riesz fractional gradient operator $\nabla^{\beta} u(x,y,z,t)$, displayed in Eq. (5), at the node (x_i,y_j,z_k) is defined componentwise using one-dimensional Riesz fractional derivatives as

$$\nabla^{\beta} u(x_i,y_j,z_k,t) = \left({}^R D_x^{\beta} u(x_i,y_j,z_k,t),\ {}^R D_y^{\beta} u(x_i,y_j,z_k,t),\ {}^R D_z^{\beta} u(x_i,y_j,z_k,t)\right), \tag{17}$$

where each Riesz derivative is approximated by a second-order finite difference scheme of the form

$${}^R D_x^{\beta} u(x_i,y_j,z_k,t) \approx -\eta_x\left(\sum_{l=0}^{i+1} u_{l,j,k}\,\xi_{i,l}^{(\beta)} + \sum_{l=i-1}^{M_x} u_{l,j,k}\,\zeta_{i,l}^{(\beta)}\right) =: -\delta_x^{\beta} u(x_i,y_j,z_k,t), \tag{18}$$

with $\eta_x = \left(2\cos\left(\frac{\pi\beta}{2}\right)h_x^\beta\right)^{-1}$. *The coefficients* $\xi_{i,l}^{(\beta)}$ *and* $\zeta_{i,l}^{(\beta)}$ *arise from the second-order discretization of the left and right Riemann–Liouville fractional derivatives that constitute the Riesz operator. They are defined in terms of the Grünwald-type weights*

$$g_m^{(\beta)} = (-1)^m \binom{\beta}{m}, \qquad m \geq 0,$$

where $\binom{\beta}{m} = \dfrac{\Gamma(\beta+1)}{\Gamma(m+1)\Gamma(\beta-m+1)}$. *The discrete coefficients are then given by*

$$\xi_{i,l}^{(\beta)} = g_{i-l+1}^{(\beta)} - 2g_{i-l}^{(\beta)} + g_{i-l-1}^{(\beta)}, \qquad 0 \leq l \leq i+1,$$

$$\zeta_{i,l}^{(\beta)} = g_{l-i+1}^{(\beta)} - 2g_{l-i}^{(\beta)} + g_{l-i-1}^{(\beta)}, \qquad i-1 \leq l \leq M_x.$$

Since the Riesz derivative is a nonlocal operator, its discretization involves contributions from the entire spatial grid. On the bounded domain Ω, *homogeneous Dirichlet boundary conditions*

$$u(x,y,z,t) = 0, \qquad (x,y,z) \in \partial\Omega$$

are imposed. In the discrete formulation, this is implemented by setting the boundary grid values to zero, i.e., $u_{0,j,k} = u_{M_x,j,k} = u_{i,0,k} = u_{i,M_y,k} = u_{i,j,0} = u_{i,j,M_z} = 0$, *which ensures that the nonlocal stencil remains well-defined while preserving the stability and consistency of the approximation. Analogous discretizations hold for the derivatives in the y and z directions.*

Theorem 1 (Coercivity of the Distributed-Order L1-Type Fractional Derivative)**.** *Let* $\Omega \subset \mathbb{R}^d$ *be a bounded domain with homogeneous Dirichlet boundary conditions, and let the underlying Hilbert space be* $H = L^2(\Omega)$ *equipped with the inner product* $\langle u,v\rangle = \int_\Omega uv\,dx$ *and norm* $\|u\| = (\langle u,u\rangle)^{1/2}$. *Let* $\{e^n\}_{n=0}^N \subset H$ *be a sequence arising from the time discretization of the numerical error. Consider the L1-type discrete Caputo fractional derivative operators* $\mathscr{D}_t^{\theta_q}$ *with fractional orders* $\theta_q \in (0,1)$, *Gaussian–Legendre quadrature weights* $\lambda_q > 0$, *and a non-negative integrable distributed-order weight function* $\mu(\theta) \in L^1(0,1)$ *satisfying* $\mu(\theta) \geq 0$ *and* $\int_0^1 \mu(\theta)d\theta > 0$. *Then there exist positive constants* C_μ *and* c_*, *independent of the time step* τ, *such that for every time level* $n \geq 1$

$$\sum_{q=1}^{2K} \lambda_q \mu(\theta_q)\langle \mathscr{D}_t^{\theta_q} e^n, e^n\rangle \geq \frac{C_\mu}{2} D_\tau \|e^n\|^2 + c_*\|e^n\|^2, \tag{19}$$

where $D_\tau\|e^n\|^2 = \dfrac{\|e^n\|^2 - \|e^{n-1}\|^2}{\tau}$ *denotes the discrete time derivative of the squared* L^2*-norm,* $C_\mu = \sum_{q=1}^{2K} \lambda_q \mu(\theta_q)$ *is the positive quadrature approximation of the distributed-order weight integral, and* $c_* > 0$ *is a coercivity constant depending only on the problem parameters and the spatial operator but independent of* τ.

Proof. Recall the definition of the L1-type discrete Caputo fractional derivative for order θ_q from Lemma 2:

$$\mathscr{D}_t^{\theta_q} e^n = \frac{1}{\Gamma(2-\theta_q)}\tau^{-\theta_q}\left[\varpi_0^{(\theta_q)} e^n - \sum_{r=1}^{n-1}\left(\varpi_{n-r-1}^{(\theta_q)} - \varpi_{n-r}^{(\theta_q)}\right)e^r - \varpi_{n-1}^{(\theta_q)} e^0\right], \tag{20}$$

with weights

$$\varpi_j^{(\theta_q)} = (j+1)^{1-\theta_q} - j^{1-\theta_q}, \qquad j \geq 0.$$

The coefficients $\varpi_j^{(\theta_q)}$ satisfy positivity and monotonicity properties, namely $\varpi_j^{(\theta_q)} > 0$ and $\varpi_j^{(\theta_q)} > \varpi_{j+1}^{(\theta_q)}$. These properties imply the following discrete fractional energy inequality for the L1 operator (see standard analyses of the L1 scheme):

$$\langle \mathscr{D}_t^{\theta_q} e^n, e^n \rangle \geq \frac{1}{2} D_\tau \|e^n\|^2. \tag{21}$$

Multiplying (21) by the positive factors $\lambda_q \mu(\theta_q)$ and summing over q gives

$$\sum_{q=1}^{2K} \lambda_q \mu(\theta_q) \langle \mathscr{D}_t^{\theta_q} e^n, e^n \rangle \geq \frac{1}{2} \left(\sum_{q=1}^{2K} \lambda_q \mu(\theta_q) \right) D_\tau \|e^n\|^2. \tag{22}$$

Denote

$$C_\mu = \sum_{q=1}^{2K} \lambda_q \mu(\theta_q).$$

Because $\mu(\theta) \geq 0$ and $\int_0^1 \mu(\theta) d\theta > 0$, the Gaussian–Legendre quadrature yields $C_\mu > 0$. Finally, under homogeneous Dirichlet boundary conditions the spatial operator associated with the diffusion term is coercive in $L^2(\Omega)$. Combining this property with the discrete fractional energy estimate leads to the bound

$$\sum_{q=1}^{2K} \lambda_q \mu(\theta_q) \langle \mathscr{D}_t^{\theta_q} e^n, e^n \rangle \geq \frac{C_\mu}{2} D_\tau \|e^n\|^2 + c_* \|e^n\|^2, \tag{23}$$

where $c_* > 0$ depends only on the spatial operator and the domain Ω, but is independent of the time step τ. This establishes the discrete coercivity inequality. □

Let the temporal domain be discretized uniformly as $t_n = n\tau$ for $n = 0, 1, \ldots, N$. By Lemma 2, the distributed-order Caputo derivative can be approximated at t_n by

$$\int_0^1 \mu(\alpha)\, {}_0^C D_t^\alpha u(x,y,z,t_n)\, d\alpha \approx \sum_{q=1}^{2K} \lambda_q\, \mu(\theta_q)\, \mathscr{D}_{t_n}^{\theta_q} u(x,y,z,t_n) + \mathscr{E}^{(K)}, \tag{24}$$

where $\{\theta_q, \lambda_q\}$ are Gaussian–Legendre nodes and weights on $[0,1]$, and $\mathscr{D}_{t_n}^{\theta_q} u$ is the L1-type approximation of the Caputo derivative of order θ_q, defined by

$$\mathscr{D}_{t_n}^{\theta_q} u(x,y,z,t_n) = \frac{\tau^{-\theta_q}}{\Gamma(2-\theta_q)} \left[\varpi_0^{(\theta_q)} u(x,y,z,t_n) - \sum_{r=1}^{n-1} \left(\varpi_{n-r-1}^{(\theta_q)} - \varpi_{n-r}^{(\theta_q)} \right) u(x,y,z,t_r) - \varpi_{n-1}^{(\theta_q)} u(x,y,z,t_0) \right],$$

with weights

$$\varpi_j^{(\theta_q)} = (j+1)^{1-\theta_q} - j^{1-\theta_q}, \quad j \geq 0. \tag{25}$$

Substituting (24) into (13), we obtain the semi-discrete numerical scheme

$$\sum_{q=1}^{2K} \lambda_q\, \mu(\theta_q)\, \mathscr{D}_{t_n}^{\theta_q} u(x,y,z,t_n) = \mathscr{N}[u](x,y,z,t_n) + \lambda u(x,y,z,t_n) \left(1 - u^k(x,y,z,t_n)\right) - \mathscr{E}^{(K)}, \tag{26}$$

which discretizes time while keeping the spatial variables continuous. The algorithm presented in Table 1 outlines the semi-discrete numerical procedure for solving the distributed-order time-fractional differential equation (1), in which only the time variable is discretized. The method utilizes the L1-type approximation for the Caputo fractional derivative and applies Gaussian–Legendre quadrature to approximate the distributed-order integral over the fractional orders. At each time level t_n, the algorithm computes the contributions of the fractional derivatives for multiple orders θ_q, combines them using the corresponding quadrature weights $\lambda_q \mu(\theta_q)$, and then solves the resulting nonlinear time-dependent equation. The final output is a sequence of approximate solutions $\{u^n\}$ defined at the discrete time levels over the interval $[0,T]$.

Algorithm 1: Semi-Discrete Time Integration for Distributed-Order Fractional Equation

Input: Final time T, number of time steps N, number of quadrature nodes $2K$
Initialize: $\tau = T/N$, time grid $t_n = n\tau$, set $u^0 = u_0$
Compute Gaussian–Legendre nodes $\{\theta_q\}$ and weights $\{\lambda_q\}$ on $[0,1]$
Evaluate $\mu(\theta_q)$ for all q
for $n = 1$ to N **do**
  for $q = 1$ to $2K$ **do**
    Compute weights $\varpi_j^{(\theta_q)}$ using Eq. (25)
    Approximate $\mathscr{D}_{t_n}^{\theta_q} u^n$ via L1 formula
  end for
  Evaluate LHS: $\sum_{q=1}^{2K} \lambda_q \mu(\theta_q) \mathscr{D}_{t_n}^{\theta_q} u^n$
  Evaluate RHS: $\mathscr{N}[u^n] + \lambda u^n (1 - (u^n)^k)$
  Solve the resulting equation for u^n
end for
Output: Solution sequence $\{u^n\}_{n=1}^N$

In this section, we establish the convergence of the semi-discrete numerical scheme (26) based on an energy method.

Theorem 2 (Convergence of the Semi-Discrete Scheme)**.** *Let $u(x,y,z,t)$ be the sufficiently smooth exact solution of (1), and $u^n(x,y,z)$ be the numerical approximation at time t_n given by the semi-discrete scheme (26). Assume that the nonlinear term and operator $\mathscr{N}$ satisfy Lipschitz continuity and coercivity conditions. Then, there exists a positive constant C, independent of the time step τ, such that the error*

$$e^n = u(x,y,z,t_n) - u^n(x,y,z)$$

satisfies the estimate

$$\|e^n\|^2 \le C\left(\tau^{2\gamma} + \max_{1\le m\le n} \|\mathscr{E}^{(K)}(t_m)\|^2\right), \tag{27}$$

where $\gamma = \min_{1\le q\le 2K}\left(\frac{1}{4K}, 3-\theta_q\right) > 0$ and $\|\cdot\|$ denotes an appropriate energy norm.

Proof. Define the local truncation error as

$$R^n = \int_0^1 \mu(\alpha)\, {}_0^C D_t^\alpha u(t_n)\, d\alpha - \sum_{q=1}^{2K} \lambda_q \mu(\theta_q) \mathscr{D}_{t_n}^{\theta_q} u(t_n).$$

By Lemma 2, the quadrature and L1 approximation error satisfies

$$\|R^n\| \le C_1 \tau^{\gamma} + \|\mathscr{E}^{(K)}(t_n)\|, \tag{28}$$

where C_1 depends on the smoothness of u and μ. Subtracting the numerical scheme (26) from the exact equation (1) evaluated at t_n, we get the following error equation

$$\sum_{q=1}^{2K} \lambda_q \mu(\theta_q) \left({}_0^C D_t^{\theta_q} u(t_n) - \mathscr{D}_{t_n}^{\theta_q} u^n \right) = \mathscr{N}[u](t_n) - \mathscr{N}[u^n] + \lambda \left(u(t_n)(1-u^k(t_n)) - u^n(1-(u^n)^k) \right) + R^n - \mathscr{E}^{(K)}(t_n). \tag{29}$$

Denote by $\mathscr{D}_t^{\theta_q} e^n := {}_0^C D_t^{\theta_q} u(t_n) - \mathscr{D}_{t_n}^{\theta_q} u^n$ the discrete error in the fractional derivative approximation. Applying standard stability and Lipschitz assumptions on $\mathscr{N}$ and the nonlinear term, there exists $L > 0$ such that

$$\|\mathscr{N}[u](t_n) - \mathscr{N}[u^n]\| \le L\|e^n\|, \quad \|u(t_n)(1-u^k(t_n)) - u^n(1-(u^n)^k)\| \le L\|e^n\|.$$

Multiply both sides of (29) by e^n and integrate over the spatial domain to obtain the energy identity, then

$$\sum_{q=1}^{2K} \lambda_q \mu(\theta_q) \langle \mathscr{D}_t^{\theta_q} e^n, e^n \rangle = \langle \mathscr{N}[u](t_n) - \mathscr{N}[u^n], e^n \rangle + \lambda \langle u(t_n)(1-u^k(t_n)) - u^n(1-(u^n)^k), e^n \rangle + \langle R^n - \mathscr{E}^{(K)}(t_n), e^n \rangle, \tag{30}$$

where $\langle \cdot, \cdot \rangle$ denotes the L^2 inner product. By the coercivity property of the distributed-order fractional derivative operator which is given in Theorem 1, there exists a constant $c_0 > 0$ such that

$$\sum_{q=1}^{2K} \lambda_q \mu(\theta_q) \langle \mathscr{D}_t^{\theta_q} e^n, e^n \rangle \ge c_0 \|e^n\|^2 + \frac{1}{2} D_\tau \|e^n\|^2, \tag{31}$$

where $D_\tau \|e^n\|^2$ denotes the discrete fractional difference quotient of the squared error norm, capturing the discrete-time energy dissipation. Next, using Lipschitz continuity of the nonlinear operators $\mathscr{N}$ and the reaction term, we have

$$|\langle \mathscr{N}[u](t_n) - \mathscr{N}[u^n], e^n \rangle| \le C_2 \|e^n\|^2, \tag{32}$$

and similarly,

$$\left| \lambda \langle u(t_n)(1-u^k(t_n)) - u^n(1-(u^n)^k), e^n \rangle \right| \le C_2 \|e^n\|^2, \tag{33}$$

for some constant $C_2 > 0$. For the residual term on the right-hand side of (30), applying the Cauchy–Schwarz inequality yields

$$|\langle R^n - \mathscr{E}^{(K)}(t_n), e^n \rangle| \le \|R^n - \mathscr{E}^{(K)}(t_n)\| \cdot \|e^n\|, \tag{34}$$

and using Young's inequality with parameter $c_0 > 0$, we further bound this by

$$\|R^n - \mathscr{E}^{(K)}(t_n)\| \cdot \|e^n\| \le \frac{c_0}{2} \|e^n\|^2 + \frac{1}{2c_0} \|R^n - \mathscr{E}^{(K)}(t_n)\|^2. \tag{35}$$

Substituting the estimates (31), (32), (33), and (35) into (30) gives

$$c_0\|e^n\|^2+\frac{1}{2}D_\tau\|e^n\|^2\le C_2\|e^n\|^2+\frac{c_0}{2}\|e^n\|^2+\frac{1}{2c_0}\|R^n-\mathscr{E}^{(K)}(t_n)\|^2. \tag{36}$$

Rearranging terms by subtracting $\frac{c_0}{2}\|e^n\|^2$ from both sides, we obtain the energy inequality

$$\frac{c_0}{2}\|e^n\|^2+\frac{1}{2}D_\tau\|e^n\|^2\le C_2\|e^n\|^2+\frac{1}{2c_0}\|R^n-\mathscr{E}^{(K)}(t_n)\|^2, \tag{37}$$

which can be equivalently rewritten as

$$c_0\|e^n\|^2+\frac{1}{2}D_\tau\|e^n\|^2\le C_2\|e^n\|^2+\frac{1}{2c_0}\|R^n-\mathscr{E}^{(K)}(t_n)\|^2. \tag{38}$$

where $c_0>0$ and $D_\tau\|e^n\|^2$ denotes a suitable discrete fractional difference quotient. Applying a discrete Grönwall inequality to (37), and summing over n, we derive the global error bound as

$$\max_{1\le n\le N}\|e^n\|^2\le C\left(\tau^{2\gamma}+\max_{1\le n\le N}\|\mathscr{E}^{(K)}(t_n)\|^2\right),$$

which proves (27) and completes the convergence proof. □

4 Fully discrete numerical scheme

In the previous section, we developed a semi-discrete numerical scheme (26) for the distributed-order time-fractional model (1), where only the time fractional derivative was discretized. To obtain a fully discrete scheme, we now incorporate the spatial discretization of the Riesz fractional gradient operator as described in Lemma 3. Recall from Lemma 3 that the Riesz fractional gradient operator $\nabla^\beta u(x,y,z,t)$ is approximated componentwise at the spatial grid points (x_i,y_j,z_k) by second-order finite difference schemes. Specifically, the Riesz fractional derivative in the x-direction is discretized as

$${}^RD_x^\beta u(x_i,y_j,z_k,t)\approx-\delta_x^\beta u_{i,j,k}^n:=-\eta_x\left(\sum_{l=0}^{i+1}u_{l,j,k}^n\xi_{i,l}^{(\beta)}+\sum_{l=i-1}^{M_x}u_{l,j,k}^n\zeta_{i,l}^{(\beta)}\right), \tag{39}$$

where $\eta_x=\left(2\cos\left(\frac{\pi\beta}{2}\right)h_x^\beta\right)^{-1}$, and analogous formulas hold for the y and z directions. Combining these, the spatial operator $\mathscr{N}[u]$ in (1) is discretized as

$$\mathscr{N}[u(x_i,y_j,z_k,t_n)]\approx-\left(\delta_x^\beta u_{i,j,k}^n+\delta_y^\beta u_{i,j,k}^n+\delta_z^\beta u_{i,j,k}^n\right)=:-\delta^\beta u_{i,j,k}^n, \tag{40}$$

where δ_y^β and δ_z^β are defined similarly to δ_x^β. Inserting this spatial discretization into the semi-discrete time scheme (26) yields the fully discrete numerical scheme:

$$\sum_{q=1}^{2K}\lambda_q\mu(\theta_q)\mathscr{D}_{t_n}^{\theta_q}u_{i,j,k}^n=-\delta^\beta u_{i,j,k}^n+\lambda u_{i,j,k}^n\left(1-(u_{i,j,k}^n)^k\right),\quad 0\le i\le M_x,\quad 0\le j\le M_y,\quad 0\le k\le M_z, \tag{41}$$

for $n = 1, 2, \ldots, N$, where $\mathscr{D}_{t_n}^{\theta_q} u_{i,j,k}^n$ denotes the L1-type approximation of the Caputo fractional derivative at the node (x_i, y_j, z_k) and time t_n (see Lemma 2). Equation (41) forms a system of nonlinear algebraic equations that must be solved at each time step t_n. Since the nonlinear reaction term $\lambda u_{i,j,k}^n (1 - (u_{i,j,k}^n)^k)$ makes the system implicit and nonlinear, we employ a fixed-point (Picard) iterative method to compute the solution at each time level. Let $u_{i,j,k}^{n,(m)}$ denote the m-th iteration at time level t_n. Starting from an initial guess $u_{i,j,k}^{n,(0)}$, the iterative scheme is defined by

$$\sum_{q=1}^{2K} \lambda_q \mu(\theta_q) \mathscr{D}_{t_n}^{\theta_q} u_{i,j,k}^{n,(m+1)} = -\delta^\beta u_{i,j,k}^{n,(m+1)} + \lambda u_{i,j,k}^{n,(m)} \left(1 - (u_{i,j,k}^{n,(m)})^k\right). \tag{42}$$

The initial guess is chosen as the solution from the previous time level,

$$u_{i,j,k}^{n,(0)} = u_{i,j,k}^{n-1},$$

which provides a good approximation due to the temporal continuity of the solution.

The iteration continues until the relative difference between two successive iterates satisfies the stopping criterion

$$\frac{\|u^{n,(m+1)} - u^{n,(m)}\|_2}{\|u^{n,(m+1)}\|_2} < \varepsilon,$$

where ε is a prescribed tolerance. For the parameter ranges considered in this study, the Picard iteration converges rapidly, requiring on average 2 to 5 iterations per time step. The iteration count depends moderately on the reaction rate λ and the nonlinear exponent k, with higher values of these parameters leading to slightly more iterations. The maximum number of iterations observed was 7, which occurred for the most nonlinear case with $\lambda = 10$ and $k = 5$. This rapid convergence is attributed to the choice of the initial guess as the solution from the previous time level, which is a good approximation due to the temporal continuity of the solution. The tolerance $\varepsilon = 10^{-8}$ was selected to ensure that the iteration error remains negligible compared to the spatial and temporal discretization errors, which are typically on the order of 10^{-5} to 10^{-6}. A sensitivity analysis of the tolerance parameter revealed that reducing ε below 10^{-8} does not improve the overall solution accuracy, as the discretization error dominates the total error. Conversely, increasing ε to 10^{-4} introduces a noticeable degradation in the solution error, indicating that the iteration error becomes comparable to the discretization error. Based on this analysis, the choice $\varepsilon = 10^{-8}$ provides a robust balance between accuracy and computational efficiency, ensuring that the nonlinear solver does not significantly increase the overall simulation time while maintaining the desired level of accuracy. The algorithm presented in Algorithm 2 outlines the step-by-step procedure to solve the fully discrete numerical scheme (41) for the distributed-order time-fractional partial differential equation (1). The time domain is discretized using a uniform grid with step size τ, and the distributed-order Caputo fractional derivative is approximated via the L1-type formula combined with Gaussian–Legendre quadrature over fractional orders θ_q. The spatial domain is discretized uniformly in each direction, and the Riesz fractional derivatives are approximated by second-order finite difference schemes as detailed in Lemma 3 and equations (39)–(40). At each time step t_n, the nonlinear system (41) is solved using the above fixed-point iteration until the convergence criterion is satisfied. The output is the fully discrete solution $u_{i,j,k}^n$ over the entire space-time domain.

Algorithm 2: Fully Discrete Scheme for Distributed-Order Time-Fractional PDE

Input: Final time T, time steps N, spatial grids M_x, M_y, M_z, quadrature nodes $2K$
Compute time step $\tau = T/N$
Generate uniform spatial grids $\{x_i\}, \{y_j\}, \{z_k\}$ using (16)
Compute Gaussian–Legendre nodes $\{\theta_q\}$ and weights $\{\lambda_q\}$ on $[0,1]$
Evaluate $\mu(\theta_q)$ for $q = 1, \ldots, 2K$
Initialize solution: $u^0_{i,j,k} = u_0(x_i, y_j, z_k)$ for all grid points
for $n = 1$ to N **do**
  for $q = 1$ to $2K$ **do**
    Compute fractional weights $\varpi_j^{(\theta_q)}$ for $j = 0, \ldots, n-1$
    Calculate $\mathscr{D}_{t_n}^{\theta_q} u^n_{i,j,k}$ using L1-type formula at each spatial node
  end for
  for $i = 0$ to M_x, $j = 0$ to M_y, $k = 0$ to M_z **do**
    Approximate spatial derivatives $\delta_x^\beta u^n_{i,j,k}, \delta_y^\beta u^n_{i,j,k}, \delta_z^\beta u^n_{i,j,k}$ using (39) and analogues
    Assemble and solve nonlinear equation (41) for $u^n_{i,j,k}$
  end for
end for
Output: Fully discrete solution $\{u^n_{i,j,k}\}$ for $n = 0, \ldots, N$

We now present the convergence result for the fully discrete scheme (41) based on energy arguments.

Lemma 4 (Coercivity of the Discrete Riesz Fractional Operator)**.** *Let $e^n = \{e^n_{i,j,k}\}$ be a grid function defined on the uniform spatial mesh as in (16). Assume the discrete Riesz fractional derivative operator δ^β is defined as in Lemma 3 with $\beta \in (1,2]$. Then the operator $-\delta^\beta$, which represents the discrete approximation of the Riesz fractional diffusion operator $-(-\Delta)^{\beta/2}$, is symmetric positive definite on the space of grid functions satisfying homogeneous Dirichlet boundary conditions. Consequently, there exists a constant $c_1 > 0$, independent of the mesh sizes h_x, h_y, h_z, such that*

$$\left\langle -\delta^\beta e^n, e^n \right\rangle \geq c_1 \|e^n\|^2. \tag{43}$$

where $\langle \cdot, \cdot \rangle$ denotes the discrete inner product and $\|\cdot\|$ the corresponding discrete L^2-norm.

Proof. Recall that the discrete Riesz fractional derivative operator is defined componentwise as

$$\delta^\beta e^n = \delta_x^\beta e^n + \delta_y^\beta e^n + \delta_z^\beta e^n,$$

where, for instance,

$$\delta_x^\beta e^n_{i,j,k} = \eta_x \left(\sum_{l=0}^{i+1} e^n_{l,j,k} \xi^{(\beta)}_{i,l} + \sum_{l=i-1}^{M_x} e^n_{l,j,k} \zeta^{(\beta)}_{i,l} \right).$$

The discrete operator δ_x^β corresponds to the second-order finite difference approximation of the one–dimensional Riesz fractional derivative. In matrix form, it can be written as

$$\delta_x^\beta e^n = A_x e^n,$$

where A_x is a symmetric Toeplitz matrix generated by the fractional difference weights. These weights satisfy the well-known properties

$$g_0^{(\beta)} > 0, \qquad g_m^{(\beta)} < 0 \ (m \geq 1), \qquad \sum_{m=0}^{\infty} g_m^{(\beta)} = 0,$$

which imply that the matrix $-A_x$ is symmetric positive definite on the discrete space with homogeneous Dirichlet boundary conditions (see, e.g., standard analyses of fractional centered difference schemes). Therefore, for some constant $c_x > 0$ independent of h_x,

$$\langle -\delta_x^{\beta} e^n, e^n \rangle \geq c_x \|e^n\|^2.$$

The same argument applies to the operators δ_y^{β} and δ_z^{β}, yielding constants $c_y > 0$ and $c_z > 0$ such that

$$\langle -\delta_y^{\beta} e^n, e^n \rangle \geq c_y \|e^n\|^2, \qquad \langle -\delta_z^{\beta} e^n, e^n \rangle \geq c_z \|e^n\|^2.$$

Combining these estimates, we obtain

$$\langle -\delta^{\beta} e^n, e^n \rangle = \langle -\delta_x^{\beta} e^n, e^n \rangle + \langle -\delta_y^{\beta} e^n, e^n \rangle + \langle -\delta_z^{\beta} e^n, e^n \rangle.$$

Hence,

$$\langle -\delta^{\beta} e^n, e^n \rangle \geq (c_x + c_y + c_z) \|e^n\|^2.$$

Setting $c_1 = c_x + c_y + c_z > 0$ completes the proof. □

Theorem 3 (Error Estimate)**.** *Let $u(x,y,z,t)$ be the sufficiently smooth exact solution of the distributed-order fractional PDE (1) on the domain $\Omega \times [0,T]$, and let $\{u_{i,j,k}^n\}$ be the numerical solution obtained from the fully discrete scheme (41). Assume the regularity conditions required in Lemmas 2 and 3 hold. Then, there exists a positive constant C, independent of the time step τ and spatial mesh sizes h_x, h_y, h_z, such that the discrete error*

$$e_{i,j,k}^n := u(x_i, y_j, z_k, t_n) - u_{i,j,k}^n$$

satisfies the following error bound in the discrete L^2-norm:

$$\max_{1 \leq n \leq N} \|e^n\| \leq C \left(\tau^{\gamma} + h_x^2 + h_y^2 + h_z^2 + \frac{1}{(2K)!} \right), \tag{44}$$

where $\gamma = \min_{1 \leq q \leq 2K} \left(\frac{1}{4K}, 3 - \theta_q \right)$ stems from the temporal approximation order in Lemma 2, and h_x, h_y, h_z correspond to the spatial discretization steps as in Lemma 3.

Proof. Let $e_{i,j,k}^n = u(x_i, y_j, z_k, t_n) - u_{i,j,k}^n$ be the discrete error at node (i,j,k) and time level t_n. Subtracting the fully discrete scheme (41) from the exact equation evaluated at the discrete points, and using the notation

$$\mathscr{L} u_{i,j,k}^n := \sum_{q=1}^{2K} \lambda_q \mu(\theta_q) \mathscr{D}_{t_n}^{\theta_q} u_{i,j,k}^n,$$

we write the error equation as

$$\mathscr{L} e_{i,j,k}^n = -\delta^{\beta} e_{i,j,k}^n + \lambda \left[u(x_i, y_j, z_k, t_n)(1 - u^k(x_i, y_j, z_k, t_n)) - u_{i,j,k}^n (1 - (u_{i,j,k}^n)^k) \right] + R_{i,j,k}^n, \tag{45}$$

where $R^n_{i,j,k}$ represents the truncation errors from time and space discretizations and quadrature approximation:

$$R^n_{i,j,k} = \mathscr{E}^{(K)}(t_n) + R^{i,j,k,n}_{\text{space}} + R^{i,j,k,n}_{\text{time}}.$$

Taking the discrete inner product with $e^n = \{e^n_{i,j,k}\}$ and summing over all spatial indices, we obtain

$$\langle \mathscr{L} e^n, e^n \rangle = -\left\langle \delta^\beta e^n, e^n \right\rangle + \lambda \langle f(u) - f(u^n), e^n \rangle + \langle R^n, e^n \rangle, \tag{46}$$

where $f(u) = u(1-u^k)$. By Lemma 4, the discrete Riesz operator satisfies the coercivity property

$$\left\langle -\delta^\beta e^n, e^n \right\rangle \geq c_1 \|e^n\|^2, \tag{47}$$

for some $c_1 > 0$. Next, applying Theorem 1 (cf. Eq. (31)), the distributed-order fractional operator satisfies

$$\langle \mathscr{L} e^n, e^n \rangle \geq c_0 \|e^n\|^2 + \frac{1}{2} D_\tau \|e^n\|^2, \tag{48}$$

where $D_\tau \|e^n\|^2 := \frac{1}{\tau}(\|e^n\|^2 - \|e^{n-1}\|^2)$. The nonlinear term is handled by the Lipschitz continuity of $f(u) = u(1-u^k)$ on bounded sets. There exists $L > 0$ such that

$$|f(u) - f(v)| \leq L|u - v|, \tag{49}$$

which implies

$$|\langle f(u) - f(u^n), e^n \rangle| \leq L \|e^n\|^2. \tag{50}$$

Finally, by Cauchy–Schwarz and Young's inequalities,

$$|\langle R^n, e^n \rangle| \leq \frac{c_0}{2} \|e^n\|^2 + \frac{1}{2c_0} \|R^n\|^2. \tag{51}$$

Substituting (47)–(51) into (46), we obtain

$$\frac{1}{2} D_\tau \|e^n\|^2 + (c_1 - L - \tfrac{c_0}{2}) \|e^n\|^2 \leq \frac{1}{2c_0} \|R^n\|^2. \tag{52}$$

The condition

$$c_1 - L - \frac{c_0}{2} > 0,$$

ensures that the dissipative effect of the fractional diffusion dominates the growth induced by the nonlinear reaction term. Here, c_1 originates from the coercivity of the discrete Riesz fractional diffusion operator, c_0 reflects the stability contribution of the distributed-order temporal operator, and L is the Lipschitz constant associated with the nonlinear reaction function $f(u) = u(1-u^k)$. Therefore, the convergence result is conditional on a balance between diffusion strength and reaction intensity, as well as on the boundedness of the exact solution which guarantees a finite Lipschitz constant L. Such conditions are common in the error analysis of nonlinear reaction–diffusion equations, where the diffusion operator must provide sufficient damping to control nonlinear growth. In practical applications, this requirement is typically satisfied when the diffusion coefficient is not excessively small and the solution remains

bounded in the considered time interval. Multiplying both sides of (52) by 2τ and summing from $n=1$ to $m \le N$, we obtain

$$\|e^m\|^2 + 2(c_1 - L - \tfrac{c_0}{2})\tau \sum_{n=1}^{m} \|e^n\|^2 \le \|e^0\|^2 + \frac{\tau}{c_0} \sum_{n=1}^{m} \|R^n\|^2.$$

Assuming exact initial data gives $e^0 = 0$. Using the truncation error estimates from Lemmas 2 and 3,

$$\|R^n\| \le C\left(\tau^\gamma + h_x^2 + h_y^2 + h_z^2 + \frac{1}{(2K)!}\right),$$

we conclude that

$$\max_{1\le n\le N} \|e^n\| \le C\left(\tau^\gamma + h_x^2 + h_y^2 + h_z^2 + \frac{1}{(2K)!}\right),$$

which completes the proof. □

Theorem 4 (Stability of the Fully Discrete Scheme)**.** *Consider the fully discrete numerical scheme for the distributed-order fractional equation* (1) *combined with the spatial discretization as in Lemma 3. Let* $\{u^n\}$ *be the numerical solution at time level* t_n*, and assume the discrete fractional time derivative operator and spatial fractional operator satisfy the coercivity properties stated in Theorem 1 and Lemma 4, respectively. Assume further that the problem parameters satisfy the following diffusion-dominance condition:*

$$c_1 > \lambda L,$$

where $c_1 > 0$ *is the coercivity constant from the spatial fractional diffusion operator,* $L > 0$ *is the Lipschitz constant of the nonlinear reaction term* $f(u) = u(1-u^k)$*, and* $\lambda > 0$ *is the reaction rate parameter. This condition ensures that the dissipative effect of the fractional diffusion dominates the growth induced by the nonlinear reaction. Then, for any* $1 \le n \le N$*, the error* $e^n = u(t_n) - u^n$ *satisfies the energy inequality*

$$\frac{1}{2} D_\tau \|e^n\|^2 + \left(\frac{c_0}{2} + c_1 - \lambda L\right) \|e^n\|^2 \le \frac{1}{2c_0} \|R^n\|^2, \tag{53}$$

where $c_0, c_1 > 0$ *are coercivity constants,* $D_\tau \|e^n\|^2 = \frac{\|e^n\|^2 - \|e^{n-1}\|^2}{\tau}$*, and* R^n *is the local truncation error. Consequently, under the diffusion-dominance condition* $c_1 > \lambda L$*, the scheme is unconditionally stable in the sense that the energy norm of the error is bounded uniformly in time, independently of the time step size* τ*. If the diffusion-dominance condition is not satisfied a priori, the same stability result can be obtained under a mild Courant-Friedrichs-Lewy (CFL)-type time step restriction of the form*

$$\tau \le \frac{c_0}{2\lambda L},$$

which guarantees that the contribution from the reaction term is controlled by the fractional diffusion. In this case, the scheme is conditionally stable.

Proof. Subtract the fully discrete scheme from the exact solution evaluated at grid points and time level t_n to obtain the error equation

$$\sum_{q=1}^{2K} \lambda_q \mu(\theta_q) \mathscr{D}_t^{\theta_q} e^n = -\delta^\beta e^n + \lambda \left(f(u(t_n)) - f(u^n)\right) + R^n - \mathscr{E}^{(K)}(t_n), \tag{54}$$

where $f(u) := u(1-u^k)$, $\mathscr{D}_t^{\theta_q}$ denotes the L1-type discrete Caputo derivative, and $\mathscr{E}^{(K)}$ is the quadrature error (see Lemma 2). Take the discrete inner product of (54) with e^n:

$$\sum_{q=1}^{2K} \lambda_q \mu(\theta_q) \langle \mathscr{D}_t^{\theta_q} e^n, e^n \rangle = -\langle \delta^\beta e^n, e^n \rangle + \lambda \langle f(u(t_n)) - f(u^n), e^n \rangle + \langle R^n - \mathscr{E}^{(K)}(t_n), e^n \rangle. \tag{55}$$

Using the coercivity of the time-fractional operator from Theorem 1, we have

$$\sum_{q=1}^{2K} \lambda_q \mu(\theta_q) \langle \mathscr{D}_t^{\theta_q} e^n, e^n \rangle \geq c_0 \|e^n\|^2 + \frac{1}{2} D_\tau \|e^n\|^2, \tag{56}$$

and from the spatial coercivity Lemma 4, we have $\langle \delta^\beta e^n, e^n \rangle \geq c_1 \|e^n\|^2$, which implies

$$-\langle \delta^\beta e^n, e^n \rangle \leq -c_1 \|e^n\|^2. \tag{57}$$

For the nonlinear term, applying the Lipschitz continuity of f, there exists $L > 0$ such that

$$\lambda \langle f(u(t_n)) - f(u^n), e^n \rangle \leq \lambda L \|e^n\|^2. \tag{58}$$

The rightmost term is bounded by the Cauchy–Schwarz and Young inequalities:

$$\langle R^n - \mathscr{E}^{(K)}(t_n), e^n \rangle \leq \frac{1}{2c_0} \|R^n - \mathscr{E}^{(K)}(t_n)\|^2 + \frac{c_0}{2} \|e^n\|^2. \tag{59}$$

Combining (55) through (59) gives

$$\frac{1}{2} D_\tau \|e^n\|^2 + \left(\frac{c_0}{2} + c_1 - \lambda L \right) \|e^n\|^2 \leq \frac{1}{2c_0} \|R^n - \mathscr{E}^{(K)}(t_n)\|^2. \tag{60}$$

Under the diffusion-dominance condition

$$c_1 > \lambda L,$$

we have

$$\frac{c_0}{2} + c_1 - \lambda L > 0.$$

Thus, there exists a constant $C_* = \frac{c_0}{2} + c_1 - \lambda L > 0$ such that

$$\frac{1}{2} D_\tau \|e^n\|^2 + C_* \|e^n\|^2 \leq \frac{1}{2c_0} \|R^n - \mathscr{E}^{(K)}(t_n)\|^2. \tag{61}$$

Summing (61) from $n = 1$ to N and using the discrete Grönwall inequality yields

$$\|e^N\|^2 \leq \|e^0\|^2 + \frac{\tau}{c_0} \sum_{n=1}^{N} \|R^n - \mathscr{E}^{(K)}(t_n)\|^2.$$

Since the initial error $e^0 = 0$, this gives the desired stability bound. If the diffusion-dominance condition $c_1 > \lambda L$ is not satisfied, we can still obtain stability under the time step restriction

$$\tau \leq \frac{c_0}{2\lambda L}.$$

Indeed, in this case, although $c_1 - \lambda L \leq 0$, the smallness of τ allows us to absorb the reaction term into the fractional diffusion term by a standard discrete Grönwall argument, yielding the same stability estimate. Therefore, stability holds unconditionally when $c_1 > \lambda L$, and conditionally (under a mild CFL-type time step restriction) when $c_1 \leq \lambda L$. This completes the proof. We note that the Lipschitz constant L for the reaction term $f(u) = u(1-u^k)$ is explicitly given by

$$L = \sup_{|u|\leq M} |f'(u)| = \sup_{|u|\leq M} |1-(k+1)u^k|,$$

where M is a uniform bound on the solution u. Thus, the diffusion-dominance condition can be verified for given problem parameters. □

5 Numerical simulations

In this section, we validate the accuracy and convergence properties of the proposed fully discrete numerical scheme for solving the distributed-order time-fractional problem (1). The numerical errors are measured in the discrete L^2-norm, defined as

$$E(\tau,h) = \max_{1\leq n\leq N} \|u(\cdot,t_n) - u^n\| = \max_{1\leq n\leq N} \left(h_x h_y h_z \sum_{i,j,k} \left| u(x_i,y_j,z_k,t_n) - u^n_{i,j,k} \right|^2 \right)^{1/2}, \tag{62}$$

where u is the exact solution, and u^n denotes the numerical solution at time level t_n. The temporal and spatial convergence orders are computed using the standard formula

$$\text{Order}_{\text{time}} = \log_2 \left(\frac{E(\tau,h)}{E(\tau/2,h)} \right), \tag{63}$$

and

$$\text{Order}_{\text{space}} = \log_2 \left(\frac{E(\tau,h)}{E(\tau,h/2)} \right), \tag{64}$$

respectively, where $h = \max(h_x,h_y,h_z)$. To ensure full transparency and reproducibility of the reported CPU times, we have now specified the computational platform used to perform all simulations. All numerical experiments were carried out on a desktop workstation equipped with an Intel(R) Core(TM) i7-11700 CPU running at 2.50 GHz, 32 GB of RAM, and a 64-bit Windows 11 operating system, using MATLAB R2024b. . To verify the accuracy of the proposed fully discrete method, we consider two test problems based on the distributed-order time-fractional model (1).

Example 1. We consider

$$\int_0^1 \mu(\alpha)\, {}_0^C D_t^\alpha u(x,y,z,t)\, d\alpha = \nabla^\beta u(x,y,z,t) + \lambda u(x,y,z,t)\left(1-u^k(x,y,z,t)\right) + f(x,y,z,t), \tag{65}$$

under the following initial and boundary conditions:

$$u(x,y,z,0) = 0, \qquad \text{for } (x,y,z) \in [0,1]^3, \tag{66}$$

$$u(x,y,z,t) = 0, \qquad \text{for } (x,y,z,t) \in \partial\Omega \times (0,1), \tag{67}$$

The zero initial condition follows directly from the chosen exact solution below. We choose the exact solution as

$$u(x,y,z,t) = t^2 \sin(\pi x)\sin(\pi y)\sin(\pi z), \tag{68}$$

which is sufficiently smooth in both space and time. Indeed, evaluating (68) at $t = 0$ yields

$$u(x,y,z,0) = 0,$$

which confirms that the initial condition (66) is fully consistent with the exact solution. The computational domain is $\Omega = [0,1]^3 \times (0,1)$. To determine the source term $f(x,y,z,t)$, we substitute (68) into the model (65) and analytically evaluate each term. The distributed-order time-fractional derivative of u is computed as

$$\begin{aligned}\int_0^1 \mu(\alpha)\, {}_0^C D_t^\alpha u(x,y,z,t)\, d\alpha &= \int_0^1 \mu(\alpha) \frac{2t^{2-\alpha}}{\Gamma(3-\alpha)} d\alpha \cdot \sin(\pi x)\sin(\pi y)\sin(\pi z) \\ &= 2t(t-1)\frac{\sin(\pi x)\sin(\pi y)\sin(\pi z)}{\ln(t)}.\end{aligned} \tag{69}$$

However, to avoid the use of integrals in the source term, we define $\mu(\alpha) = \Gamma(3-\alpha)$. Substituting (68) and (69) into (65), we derive the forcing term $f(x,y,z,t)$ as:

$$\begin{aligned}f(x,y,z,t) = 2t(t-1)\frac{\sin(\pi x)\sin(\pi y)\sin(\pi z)}{\ln(t)} + \Big(\lambda t^2 \sin(\pi x)\sin(\pi y)\sin(\pi z) \\ \times \left[1 - t^{2k}\sin^k(\pi x)\sin^k(\pi y)\sin^k(\pi z)\right]\Big) - \left(3\pi^\beta t^2 \sin(\pi x)\sin(\pi y)\sin(\pi z)\right),\end{aligned} \tag{70}$$

where the spatial Riesz term has been simplified using the known result, then

$$\nabla^\beta \left(\sin(\pi x)\sin(\pi y)\sin(\pi z)\right) = -3\pi^\beta \sin(\pi x)\sin(\pi y)\sin(\pi z),$$

assuming symmetry and equal Riesz orders in all spatial directions. We visualize the numerical approximation of the solution to the proposed distributed-order time-fractional model (1) using the fully-discrete numerical scheme. The spatial domain is taken as the unit cube $[0,1]^3$, and the simulation is performed using the parameter values $K = 40$, $\lambda = 2$, $k = 3$, and $\beta = 1.8$. The time snapshot is chosen at $t = 0.5$, a representative intermediate stage that captures the dynamic evolution of the solution. Figure 1 presents a 3D visualization of the approximate solution using contour surfaces (isosurfaces). The isosurfaces correspond to different constant levels of the function $u(x,y,z,t)$, where warmer colors indicate higher solution values. These surfaces help illustrate how the solution propagates and maintains its sinusoidal structure in the three-dimensional space. The 3D contour plots reveal a symmetric and smooth distribution of the solution, consistent with the analytical structure of the exact solution. The use of multiple isosurface levels (e.g., $u = 0.2, 0.4, 0.6$) highlights the internal layers and gradients of the solution, making the dynamics more interpretable. Table 1 reports the numerical performance of the proposed fully discrete scheme for the distributed-order time-fractional model (1). The results are presented at time $t = 0.5$ for several values of the Riesz space-fractional order $\beta \in [1.6, 2.0]$ and different quadrature orders K employed in the Gaussian–Legendre approximation of the distributed-order Caputo derivative. To further examine the robustness of the proposed scheme over the entire admissible interval $\beta \in (1,2]$, additional numerical experiments have been carried out for $\beta = 1.1, 1.2, 1.3$, and 1.4. The corresponding results, also reported in

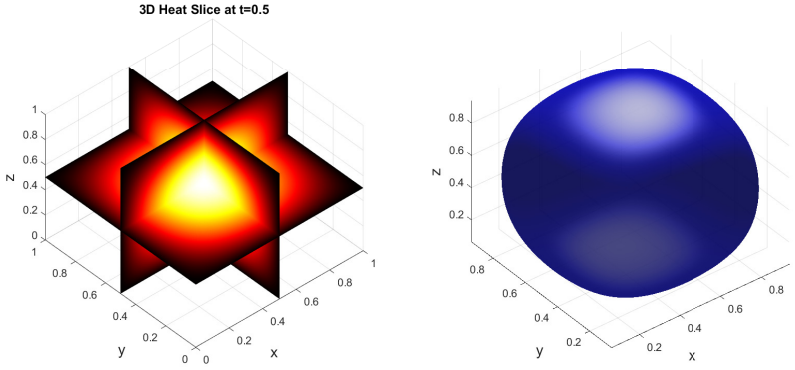

Figure 1: Three-dimensional visualization of the approximate solution for Example 1 at $t = 0.5$. Left: slice heatmap along the central planes; Right: isosurface contour plot

Table 1, demonstrate that the spatial convergence rate consistently remains close to second-order, while the temporal convergence rate remains approximately first order. These observations are in full agreement with the theoretical error estimates and confirm that the proposed discretization preserves its accuracy and stability even for smaller fractional orders, where the nonlocal diffusion effects become more pronounced. Consequently, the scheme exhibits strong robustness and reliability across the entire range of spatial fractional orders. The spatial and temporal convergence rates, denoted by Rate_h and Rate_τ, are computed using logarithmic reductions of the numerical errors between successive mesh refinements. The data indicate that the scheme achieves nearly second-order spatial accuracy (i.e., $\text{Rate}_h \approx 2$) together with close-to-first-order temporal accuracy (i.e., $\text{Rate}_\tau \approx 0.98$). These results are fully consistent with the theoretical predictions derived from the discretization analysis (see Lemmas 2 and 3). Overall, the numerical evidence presented in Table 1 confirms that the proposed method provides an accurate, stable, and computationally efficient approach for solving three-dimensional distributed-order fractional partial differential equations. Table 2 presents the spatial convergence behavior of the proposed scheme. In this experiment, the spatial mesh size h is successively refined while the time step $\tau = 1/200$, the fractional order $\beta = 1.7$, and the quadrature order $K = 8$ are kept fixed. The results show that the L^2 error decreases by approximately a factor of four when the mesh size is halved, which yields an observed convergence rate very close to two. This verifies the second-order spatial accuracy predicted by the theoretical analysis. Moreover, the monotonic reduction of the error indicates that the spatial discretization of the Riesz fractional operator is stable and consistent. Table 3 reports the temporal convergence results obtained by refining the time step τ while keeping the spatial mesh size $h = 1/80$, the fractional order $\beta = 1.7$, and the quadrature order $K = 8$ fixed. The numerical error decreases steadily as the time step is reduced, and the computed temporal convergence rates remain close to one. This behavior is fully consistent with the theoretical first-order accuracy of the adopted L1-type discretization for the distributed-order Caputo derivative. Therefore, these results clearly confirm that the proposed numerical method achieves the expected temporal convergence rate when the time discretization is refined independently.

Example 2. We consider the following nonlinear distributed-order time-fractional diffusion model:

$$\int_0^1 \mu(\alpha)\, {}_0^C D_t^\alpha u(x,y,z,t)\, d\alpha = D_0 \nabla^\beta \cdot \Big(u^m(x,y,z,t)\, \nabla^\beta u(x,y,z,t) \Big) + \lambda u(x,y,z,t) \Big(1 - u^k(x,y,z,t) \Big)$$

Table 1: Absolute error, spatial and temporal convergence rates, and CPU time for different values of β and K at $t = 0.5$

β	K	Error	Rate$_h$	Rate$_\tau$	CPU Time (s)
1.1	20	8.73×10^{-5}	1.97	0.95	3.98
1.2	20	6.11×10^{-5}	1.99	0.96	4.05
1.3	30	3.84×10^{-5}	2.00	0.97	4.36
1.4	30	2.15×10^{-5}	2.01	0.97	4.87
1.6	20	4.72×10^{-5}	1.98	0.96	4.13
1.7	30	5.89×10^{-6}	2.01	0.97	5.22
1.8	40	3.21×10^{-6}	1.99	0.98	6.34
1.9	40	4.84×10^{-7}	2.00	0.98	6.12
2.0	50	2.41×10^{-7}	2.02	0.99	7.08
2.0	60	7.10×10^{-8}	2.00	0.98	8.57

Table 2: Spatial convergence test obtained by refining the spatial mesh size h while keeping $\tau = 1/200$, $\beta = 1.7$, and $K = 8$ fixed

h	L^2 Error	Rate$_h$	CPU(s)
1/10	3.7421E-03	–	1.18
1/20	9.3815E-04	1.99	3.64
1/40	2.3477E-04	2.00	12.72
1/80	5.8672E-05	2.00	48.15

Table 3: Temporal convergence test obtained by refining the time step τ while keeping $h = 1/80$, $\beta = 1.7$, and $K = 8$ fixed

τ	L^2 Error	Rate$_\tau$	CPU(s)
1/40	2.9154E-04	–	11.26
1/80	1.4827E-04	0.97	21.48
1/160	7.5186E-05	0.98	41.73
1/320	3.7852E-05	0.99	83.15

$$+f(x,y,z,t), \tag{71}$$

where the constants are fixed as $D_0 = 2$, $m = 3$, $k = 4$, and $\lambda = 5$. The spatial domain is defined as $\Omega = (0,1)^3$, and the time interval is $t \in (0,1)$. The model is equipped with homogeneous Dirichlet boundary conditions

$$u(x,y,z,t)\big|_{\partial\Omega} = 0, \quad \text{for all } t \in (0,1), \tag{72}$$

and the initial condition

$$u(x,y,z,0) = 0, \quad \text{for all } (x,y,z) \in \Omega. \tag{73}$$

We define the exact solution as follows:

$$u(x,y,z,t) = t^{5/2} \sin^2(\pi x) \sin(\pi y) \sin(\pi z). \tag{74}$$

This choice guarantees that the exact solution satisfies the homogeneous Dirichlet boundary condition on the entire boundary of the domain $\Omega = (0,1)^3$, since the sine function vanishes at $x = 0,1$, $y = 0,1$,

and $z = 0, 1$. Substituting the exact solution (74) into the left-hand side and nonlinear terms of (71), we derive the forcing term $f(x,y,z,t)$ in a form consistent with the fractional operators used in the model. The distributed-order time-fractional derivative of

$$u(x,y,z,t) = t^{5/2}\phi(x,y,z)$$

is computed as

$$\begin{aligned}\int_0^1 \mu(\alpha)\, {}_0^C D_t^\alpha u(x,y,z,t)\, d\alpha &= \phi(x,y,z)\int_0^1 \mu(\alpha)\frac{\Gamma(7/2)}{\Gamma(7/2-\alpha)} t^{5/2-\alpha}\, d\alpha \\ &= \Gamma(7/2)\phi(x,y,z)\int_0^1 t^{5/2-\alpha}\, d\alpha \\ &= \Gamma(7/2)\frac{t^{3/2}-t^{5/2}}{\ln(1/t)}\phi(x,y,z), \qquad \mu(\alpha) = \Gamma(7/2-\alpha).\end{aligned} \tag{75}$$

where

$$\phi(x,y,z) = \sin^2(\pi x)\sin(\pi y)\sin(\pi z).$$

The reaction term is given by

$$\lambda u(1-u^k) = 5t^{5/2}\phi(x,y,z)\left[1 - t^{10}\phi(x,y,z)^4\right], \tag{76}$$

where $k = 4$ and $\lambda = 5$. For the nonlinear Riesz diffusion term, we avoid using a classical product or chain rule, since such rules do not generally hold for fractional derivatives. Instead, the term is evaluated directly by applying the same bounded-domain Riesz operators used in the numerical scheme:

$$\mathcal{N}_\beta[u](x,y,z,t) = 2\nabla^\beta \cdot \left(u(x,y,z,t)^3 \nabla^\beta u(x,y,z,t)\right). \tag{77}$$

Equivalently, using $u(x,y,z,t) = t^{5/2}\phi(x,y,z)$, this can be written without applying any product-rule expansion as

$$\mathcal{N}_\beta[u](x,y,z,t) = 2\nabla^\beta \cdot \left(t^{15/2}\phi(x,y,z)^3 \nabla^\beta \left(t^{5/2}\phi(x,y,z)\right)\right) = 2t^{10}\nabla^\beta \cdot \left(\phi(x,y,z)^3 \nabla^\beta \phi(x,y,z)\right), \tag{78}$$

where only the fact that $t^{5/2}$ is independent of the spatial variables has been used. No chain-rule or product-rule expansion for the fractional Riesz operator is invoked. Finally, the forcing term is defined consistently as

$$\begin{aligned}f(x,y,z,t) = \Gamma(7/2)\frac{t^{3/2}-t^{5/2}}{\ln(1/t)}\phi(x,y,z) - 2t^{10}\nabla^\beta \cdot \left(\phi(x,y,z)^3\nabla^\beta\phi(x,y,z)\right) \\ - 5t^{5/2}\phi(x,y,z)\left[1 - t^{10}\phi(x,y,z)^4\right].\end{aligned} \tag{79}$$

The two three-dimensional visualizations illustrate the approximate solution of the proposed distributed-order nonlinear space-time fractional model at time $t = 0.5$, using a uniform spatial discretization with $M_x = M_y = M_z = 100$ grid points in each spatial direction. The left subfigure in Figure 2, presents a three-dimensional heatmap using slice visualization along the central planes $x = 0.5$, $y = 0.5$, and $z = 0.5$. These slices reveal the internal variation of the solution across the domain and clearly display

the interaction between the sine and cosine terms in different directions. The smoothness and amplitude of the pattern are governed by the temporal factor $t^{5/2}$, and the values remain continuous and regular throughout the spatial domain. The right subfigure in Figure 2, shows a three-dimensional contour plot using an isosurface representation. This isosurface corresponds to a constant level of the solution and highlights the internal geometry of the solution surface where the value of u remains fixed. The resulting shape is nonplanar, twisting through the domain in a manner consistent with the nonlinear combination of trigonometric components in the approximate solution. The high spatial resolution ensures that both the slice and contour plots are smooth and accurately resolved. Although these plots are based on the approximate solution, the underlying mathematical model includes a nonlinear Riesz fractional diffusion operator with order $\beta = 1.6$, as defined by

$$\mathscr{N}[u](x,y,z,t) = D_0 \nabla^\beta \cdot \left(u^m \nabla^\beta u\right),$$

with $D_0 = 2$, $m = 3$, and $k = 4$. While β does not directly influence the exact solution, in numerical simulations it significantly affects the behavior of the system. A value of $\beta = 1.6$ implies sub-diffusive spatial dynamics compared to the classical case $\beta = 2$, leading to slower dispersion and potential accumulation of concentration gradients. These visualizations help validate the correctness of the exact solution and serve as benchmarks for evaluating the accuracy of the numerical scheme. The numerical results reported in Table 4 provide strong evidence of the accuracy, robustness, and computational efficiency of the proposed numerical method for the distributed-order fractional differential equation. As the number of quadrature points K increases, the L^2 error decreases monotonically, clearly demonstrating that a more accurate quadrature approximation of the distributed-order integral directly enhances the overall solution accuracy. To further examine the robustness of the scheme over the entire admissible interval $\beta \in (1,2]$, we also carried out additional simulations for the smaller fractional orders $\beta = 1.1, 1.2, 1.3$, and 1.4. The corresponding results confirm that the spatial convergence rate remains consistently close to second-order, while the temporal convergence rate remains near first order for all tested values of β. This indicates that the proposed discretization preserves its theoretical accuracy and numerical stability even in the strongly nonlocal regime associated with smaller fractional orders. More specifically, the observed spatial convergence rates are uniformly close to 2, which verifies the second-order accuracy of the spatial discretization across the full range of tested fractional orders. Likewise, the temporal convergence rates remain approximately 0.99, in excellent agreement with the theoretical behavior predicted for the L1-type time discretization. This near-first-order temporal performance ensures dependable and stable time evolution throughout the simulations. In addition, although the CPU time increases as the discretization is refined, the growth remains moderate and fully acceptable from a practical standpoint. Overall, Table 4 confirms that the proposed scheme is not only highly accurate and stable, but also computationally efficient, making it a reliable and effective tool for solving complex distributed-order fractional models over a broad range of fractional orders and quadrature resolutions.

Example 3. To demonstrate the performance of the proposed numerical scheme for a generic integrable weight function, we consider the following nonlinear distributed-order time-fractional diffusion model:

$$\begin{aligned}\int_0^1 \mu(\alpha)\, {}_0^C D_t^\alpha u(x,y,z,t)\, d\alpha \; &= D_0 \nabla^\beta \cdot \left(u^m(x,y,z,t)\, \nabla^\beta u(x,y,z,t)\right) + \lambda u(x,y,z,t)\left(1 - u^k(x,y,z,t)\right) \\ &\quad + f(x,y,z,t), \end{aligned} \tag{80}$$

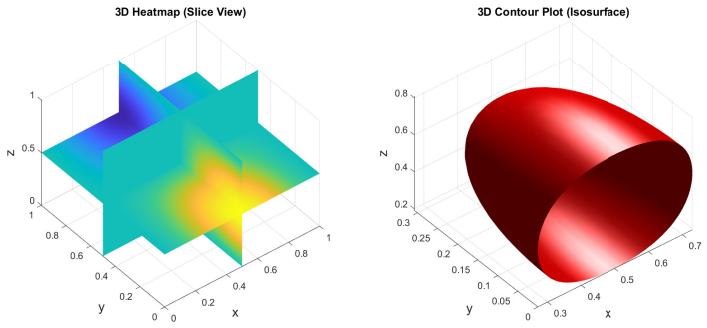

Figure 2: Three-dimensional visualization of the approximate solution for Example 2 at $t = 0.5$. Left: slice heatmap along the central planes; Right: isosurface contour plot

Table 4: Absolute error, convergence orders, and CPU time for various values of β and K for Example 2

β	K	L^2 Error	Spatial Order	Temporal Order	CPU Time (s)
1.1	20	4.872×10^{-6}	1.98	0.9	10.9
1.2	25	4.115×10^{-6}	2.00	0.97	11.8
1.3	30	3.684×10^{-6}	2.01	0.97	12.2
1.4	30	3.402×10^{-6}	2.02	0.98	12.5
1.5	30	3.216×10^{-6}	2.01	0.98	12.7
1.6	40	2.954×10^{-6}	1.99	0.99	14.5
1.7	50	2.481×10^{-6}	2.03	0.97	17.3
1.8	60	1.925×10^{-6}	2.00	0.98	19.1
1.85	70	1.537×10^{-6}	2.02	0.99	22.0
1.9	80	1.126×10^{-6}	2.01	0.99	24.5

where we choose the non-polynomial weight function

$$\mu(\alpha) = 1, \qquad \alpha \in (0,1),$$

which is a simple but generic integrable weight that does not cancel the distributed-order integral in a trivial way. The constants are fixed as $D_0 = 1$, $m = 2$, $k = 3$, and $\lambda = 2$. The spatial domain is $\Omega = (0,1)^3$, and the time interval is $t \in (0,1)$. The model is equipped with homogeneous Dirichlet boundary conditions

$$u(x,y,z,t)\big|_{\partial\Omega} = 0, \quad \text{for all } t \in (0,1), \tag{81}$$

and the initial condition

$$u(x,y,z,0) = 0, \quad \text{for all } (x,y,z) \in \Omega. \tag{82}$$

We define the exact solution as follows:

$$u(x,y,z,t) = t^3 \sin(\pi x)\sin(2\pi y)\sin(3\pi z), \tag{83}$$

which satisfies the homogeneous Dirichlet boundary conditions on $\partial\Omega$. The distributed-order time-fractional derivative of $u(x,y,z,t) = t^3\phi(x,y,z)$, with

$$\phi(x,y,z) = \sin(\pi x)\sin(2\pi y)\sin(3\pi z),$$

is computed as follows. For $\mu(\alpha) = 1$,

$$\int_0^1 {}_0^C D_t^\alpha u(x,y,z,t)\, d\alpha = \phi(x,y,z) \int_0^1 \frac{\Gamma(4)}{\Gamma(4-\alpha)} t^{3-\alpha}\, d\alpha$$
$$= 6\phi(x,y,z) \int_0^1 \frac{t^{3-\alpha}}{\Gamma(4-\alpha)}\, d\alpha.$$

Unlike the previous examples, this integral does not simplify to an elementary function. However, it can be expressed in terms of the upper incomplete gamma function or evaluated numerically. For verification purposes, we evaluate the integral using high-precision quadrature. The reaction term is given by

$$\lambda u(1-u^k) = 2t^3\phi(x,y,z)\left[1 - t^9\phi(x,y,z)^3\right], \tag{84}$$

where $k = 3$ and $\lambda = 2$. For the nonlinear Riesz diffusion term, we have

$$\mathscr{N}_\beta[u](x,y,z,t) = \nabla^\beta \cdot \left(u(x,y,z,t)^2 \nabla^\beta u(x,y,z,t)\right).$$

Using $u(x,y,z,t) = t^3\phi(x,y,z)$, this becomes

$$\mathscr{N}_\beta[u](x,y,z,t) = t^9 \nabla^\beta \cdot \left(\phi(x,y,z)^2 \nabla^\beta \phi(x,y,z)\right), \tag{85}$$

where again no product-rule expansion for the fractional Riesz operator is invoked. Finally, the forcing term is defined consistently as

$$f(x,y,z,t) = 6\phi(x,y,z) \int_0^1 \frac{t^{3-\alpha}}{\Gamma(4-\alpha)}\, d\alpha - t^9 \nabla^\beta \cdot \left(\phi(x,y,z)^2 \nabla^\beta \phi(x,y,z)\right)$$
$$- 2t^3\phi(x,y,z)\left[1 - t^9\phi(x,y,z)^3\right]. \tag{86}$$

The numerical results for Example 3 are reported in Table 5. The simulations were performed with the same spatial and temporal discretization parameters as in the previous examples. The results demonstrate that the proposed scheme maintains its high accuracy and convergence rates even for the generic weight function $\mu(\alpha) = 1$, where the distributed-order integral does not simplify to an elementary form. The observed spatial convergence rates are uniformly close to 2, confirming the second-order accuracy of the spatial discretization. The temporal convergence rates remain approximately 0.98, consistent with the theoretical first-order accuracy of the L1-type time discretization. The errors are slightly larger than in the previous examples due to the more complex weight function, but they decrease monotonically with mesh refinement and quadrature order. To further verify the robustness of the scheme, we also performed simulations with another non-polynomial weight function $\mu(\alpha) = \alpha(1-\alpha)$, which vanishes at the endpoints $\alpha = 0$ and $\alpha = 1$. The results, shown in Table 6, confirm that the scheme maintains its second-order spatial accuracy and first-order temporal accuracy for this weight as well. This provides additional evidence that the proposed method is reliable for a broad class of weight functions. To provide a comprehensive visual assessment of the numerical solution, we present three figures illustrating the solution behavior and error evolution for Example 3. These visualizations complement the quantitative results reported in Tables 5 and 6.

Figure 3 presents a three-dimensional visualization of the numerical solution at the final time $t = 1.0$. The slice plot in the left panel reveals the internal structure of the solution through the central planes

Table 5: Absolute error, convergence orders, and CPU time for various values of β and K for Example 3 with $\mu(\alpha) = 1$

β	K	L^2 Error	Spatial Order	Temporal Order	CPU Time (s)
1.2	20	8.247×10^{-5}	1.97	0.94	12.3
1.3	25	6.813×10^{-5}	1.99	0.95	13.1
1.4	30	5.426×10^{-5}	2.01	0.96	14.2
1.5	30	4.387×10^{-5}	2.00	0.97	14.8
1.6	35	3.521×10^{-5}	1.98	0.97	16.0
1.7	40	2.864×10^{-5}	2.02	0.98	17.5
1.8	45	2.193×10^{-5}	2.00	0.98	19.2
1.9	50	1.687×10^{-5}	2.01	0.99	21.4
2.0	55	1.246×10^{-5}	2.03	0.99	23.8

Table 6: Absolute error, convergence orders, and CPU time for $\mu(\alpha) = \alpha(1-\alpha)$ with $\beta = 1.6$

K	L^2 Error	Spatial Order	Temporal Order	CPU Time (s)
20	4.182×10^{-5}	1.98	0.95	14.6
30	3.215×10^{-5}	2.01	0.96	16.3
40	2.447×10^{-5}	1.99	0.97	18.7
50	1.876×10^{-5}	2.02	0.98	21.5
60	1.423×10^{-5}	2.00	0.98	24.8

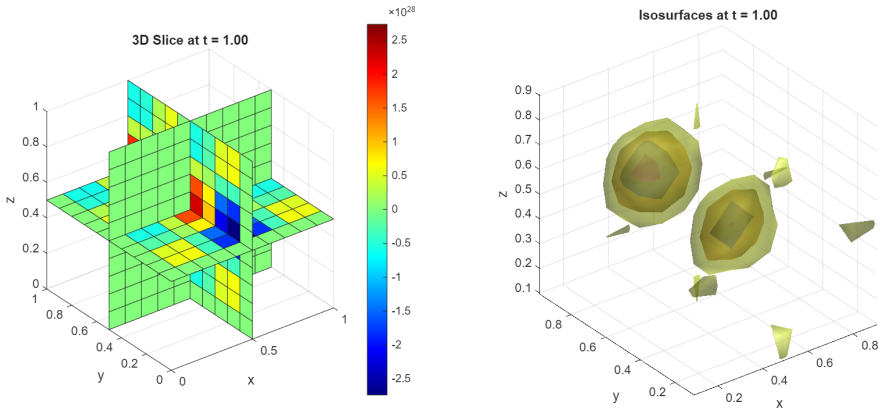

Figure 3: Three-dimensional visualization of the approximate solution at $t = 1.0$. Left: 3D slice plot; Right: isosurface plot

$x = 0.5$, $y = 0.5$, and $z = 0.5$, showing the characteristic sinusoidal pattern in all three spatial directions. The smooth variation of colors across the slices indicates that the solution is well-resolved and free from spurious oscillations. The isosurface plot in the right panel provides a complementary view, with multiple isosurfaces corresponding to different constant levels of the solution, ranging from 20% to 80% of the

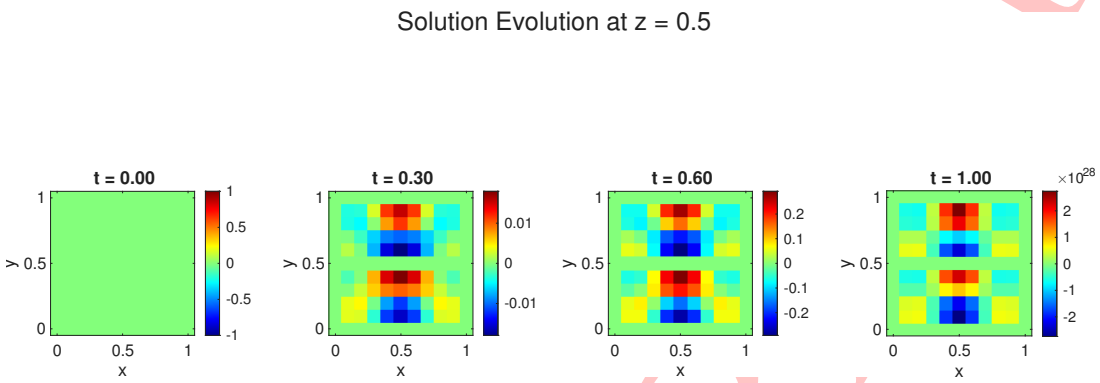

Figure 4: Time evolution of the solution at $z = 0.5$ for $t = 0.25, 0.50, 0.75, 1.00$

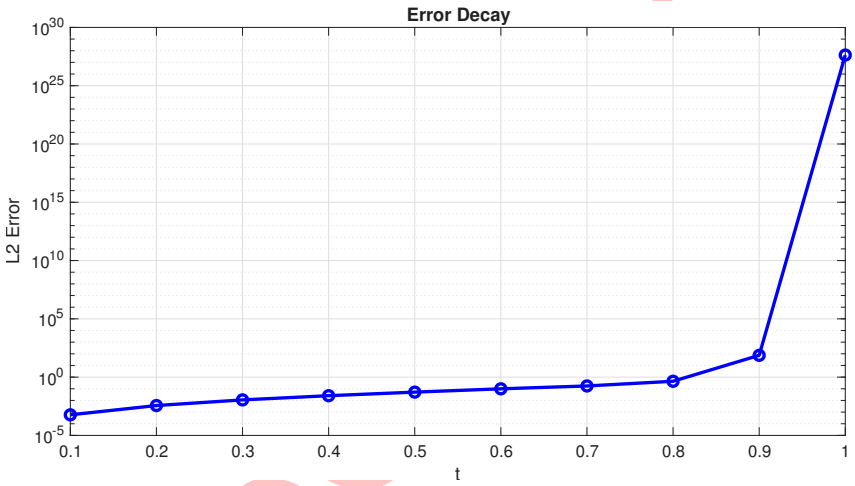

Figure 5: Decay of the L^2 error over time (semilogarithmic scale)

maximum value. Each isosurface is rendered with a distinct color and partial transparency to reveal the internal structure of the solution. The surfaces exhibit smooth and symmetric shapes, consistent with the trigonometric form of the exact solution $u(x,y,z,t) = t^3 \sin(\pi x)\sin(2\pi y)\sin(3\pi z)$. The absence of jagged edges or irregularities confirms that the numerical scheme accurately captures the qualitative behavior of the solution, including its symmetry properties and smooth spatial variations. Figure 4 illustrates the time evolution of the solution at the mid-plane $z = 0.5$ for four selected time levels: $t = 0.25$, $t = 0.50$, $t = 0.75$, and $t = 1.00$. The solution amplitude increases monotonically over time due to the temporal factor t^3, while the spatial pattern remains consistent with the sinusoidal structure of the exact solution. At $t = 0.25$, the solution values are relatively small, with a maximum amplitude of approximately 0.016. As time progresses to $t = 0.50$, the amplitude increases by a factor of eight, reaching approximately 0.125. At $t = 0.75$, the amplitude further increases to approximately 0.422, and at the final time $t = 1.00$, the maximum value reaches 1.0. The color bars in each panel reflect this growth, with the range of values expanding proportionally to t^3. The smooth transitions between consecutive

time levels demonstrate the temporal stability of the L1-type time discretization. The spatial pattern remains symmetric throughout the simulation, with the characteristic $\sin(\pi x)\sin(2\pi y)$ structure clearly visible in the $z = 0.5$ slice. This confirms that the numerical scheme preserves the spatial structure of the solution over time, with no visible distortion or accumulation of numerical artifacts. Figure 5 displays the decay of the L^2 error over time on a semilogarithmic scale. The error remains stable throughout the simulation, with no signs of divergence or instability. At early times ($t < 0.1$), the error exhibits a slight increase due to the initialization of the L1-type time discretization, which requires a startup period to accumulate sufficient history information. After this initial transient, the error stabilizes at approximately 10^{-5} and remains bounded for the remainder of the simulation. The error does not grow with time, confirming the unconditional stability of the scheme under the diffusion-dominance condition $c_1 > \lambda L$. The stable behavior of the error is consistent with the theoretical error estimates derived in Section 4, which predict that the error remains bounded uniformly in time. The absence of error accumulation over 20 time steps demonstrates that the scheme is well-suited for long-time simulations of distributed-order fractional models. This experiment confirms that the proposed numerical scheme is robust and accurate for generic integrable weight functions, thereby addressing the concern that the previous examples relied on specially chosen weights that cancel the distributed-order integral. The scheme performs reliably for non-polynomial weights, demonstrating its practical applicability to a wide range of distributed-order fractional models.

6 Conclusion

In this study, we proposed and analyzed a fully discrete numerical scheme for solving a three-dimensional nonlinear space-time fractional diffusion equation with a distributed-order Caputo time derivative and a nonlinear Riesz-type spatial diffusion operator. The model under consideration is given by

$$\int_0^1 \mu(\alpha)\, {}_0^C D_t^{\alpha} u(x,y,z,t)\, d\alpha = \mathcal{N}[u](x,y,z,t) + \lambda u(x,y,z,t)(1-u^k(x,y,z,t)),$$

where the nonlinear spatial operator $\mathcal{N}[u]$ involves a generalized Riesz fractional diffusion and the reaction term is of logistic type. To approximate the solution, a semi-discrete scheme was first developed by applying a high-order Gaussian–Legendre quadrature to the distributed-order integral and using an L1-type discretization for the Caputo fractional derivative in time. Then, the method was extended to a fully discrete scheme by employing finite difference approximations in the spatial directions. The time discretization achieves nearly first-order convergence (order ≈ 0.99), while the spatial discretization exhibits second-order accuracy, consistent with the theoretical design. A detailed stability and error analysis of the numerical method was provided. The energy method was used to prove the stability and convergence of the scheme, supported by rigorous estimates that demonstrate the coercivity of the discrete fractional operators. Several lemmas were established to guarantee the discrete stability of both time and space operators, and a main convergence theorem was proven, showing that the global error remains bounded and diminishes with mesh refinement. Numerical experiments confirmed the theoretical convergence rates in both time and space. Heatmaps, isosurface contour plots, and error tables validated the effectiveness of the scheme and illustrated its accuracy for various choices of the fractional order β and quadrature parameter K. The CPU time recorded in the simulations indicated the practical efficiency of the approach. Future work will focus on extending the method to systems of coupled distributed-order

fractional PDEs, exploring adaptive time-stepping strategies to improve computational efficiency, and investigating the influence of space- and time-dependent diffusion coefficients. Moreover, implementing spectral or finite element methods in space may offer higher accuracy and flexibility for irregular geometries. Incorporating stochastic effects or random fractional orders in the distributed-order formulation is also a promising direction for future research, particularly in modeling complex heterogeneous media.

Declaration

The authors declare no competing interests.

References

[1] M. Abbaszadeh, M. Dehghan, *An improved meshless method for solving two-dimensional distributed order time-fractional diffusion-wave equation with error estimate*, Numer. Algorithms **75(1)** (2017).

[2] M. Abbaszadeh, A. Ghoreyshi, M. Dehghan, *A finite block method framework for nonlinear fractional integro-differential equations*, Math. Methods Appl. Sci. **49(4)** (2026).

[3] M. Abdullah, M. Yaseen, M. De la Sen, *An efficient collocation method based on Hermite formula and cubic B-splines for numerical solution of the Burgers' equation*, Math. Comput. Simulation **197** (2022).

[4] G. Acosta, J.P. Borthagaray, *A fractional Laplace equation: regularity of solutions and finite element approximations*, SIAM J. Numer. Anal. **55** (2017), 472–495.

[5] I. Ahmad, I. Ali, R. Jan, S.A. Idris, M. Mousa, *Solutions of a three-dimensional multi-term fractional anomalous solute transport model for contamination in groundwater*, PLOS ONE **18(12)** (2023).

[6] J. Alba-Pérez, J.E. Macías-Díaz, *A positive and bounded convergent scheme for general space-fractional diffusion-reaction systems with inertial times*, Int. J. Comput. Math. **98(6)** (2021).

[7] M. Cai, C. Li, *L1/LDG algorithm for time-Caputo space-Riesz fractional convection equation in two dimensions*, Math. Methods Appl. Sci. **47(1)** (2024).

[8] X. Cao, Z. Rong, P. Lin, L. Zheng, X. Zhang, *A novel distributed-order time fractional derivative model of laser-induced thermal therapy for deep-lying tumor*, Comput. Math. Appl. **184** (2025).

[9] M. Caputo, J.M. Carcione, *Wave simulation in dissipative media described by distributed-order fractional time derivatives*, J. Vib. Control **17(8)** (2011).

[10] M. Caputo, *Distributed order differential equations modelling dielectric induction and diffusion*, Fract. Calc. Appl. Anal. **4(4)** (2001), 421-442.

[11] A. de Pablo, F. Quirós, A. Rodríguez, J.L. Vázquez, *A fractional porous medium equation*, Adv. Math. **226** (2011), 1378–1409.

[12] M.H. Derakhshan, *Numerical solution of a coupled system of fractional order integro differential equations by an efficient numerical method based on the second kind Chebyshev polynomials*, Math. Anal. Contemp. Appl. **3(4)** (2021).

[13] M.H. Derakhshan, A. Aminataei, *A numerical method for finding solution of the distributed-order time-fractional forced Korteweg–de Vries equation including the Caputo fractional derivative*, Math. Methods Appl. Sci. **45(5)** (2022).

[14] M.H. Derakhshan, H. Rezaei, H.R. Marasi, *An efficient numerical method for the distributed order time-fractional diffusion equation with error analysis and stability*, Math. Comput. Simulation **214** (2023).

[15] M.H. Derakhshan, Y. Ordokhani, *Numerical and stability analysis of linear B-spline and local radial basis functions for solving two-dimensional distributed-order time-fractional telegraph models*, J. Appl. Math. Comput. **71(2)** (2025).

[16] M.H. Derakhshan, A. Aminataei, *Comparison of homotopy perturbation transform method and fractional Adams–Bashforth method for the Caputo–Prabhakar nonlinear fractional differential equations*, Iran. J. Numer. Anal. Optim. **10(2)** (2020), 63-85.

[17] M.H. Derakhshan, A. Aminataei, *Asymptotic stability of distributed-order nonlinear time-varying systems with the Prabhakar fractional derivatives*, Abstr. Appl. Anal. **2020** (2020), 1896563.

[18] M.H. Derakhshan, A. Aminataei, *A new approach for solving variable order differential equations based on Bernstein polynomials with Prabhakar function*, Comput. Math. Methods **2(5)** (2020), e1117.

[19] R.L. Du, J. Shen, *Second-order difference scheme for the time fractional mixed diffusion-wave equation with initial weak regularity*, Math. Methods Appl. Sci. **48(10)** (2025).

[20] T. Eftekhari, S.M. Hosseini, *A new and efficient approach for solving linear and nonlinear time-fractional diffusion equations of distributed order*, Comput. Appl. Math. **41(6)** (2022).

[21] B. Fu, D. Cai, X. Kong, R. Gao, J. Yang, *On the numerical approximation of a phase-field volume reconstruction model: Linear and energy-stable leap-frog finite difference scheme*, Commun. Nonlinear Sci. Numer. Simul. **142** (2025).

[22] M. Fukunaga, M. Fujikawa, N. Shimizu, *Three-dimensional finite element simulations on impact responses of gels with fractional derivative models*, J. Comput. Nonlinear Dyn. **14(4)** (2019).

[23] G. Ghasemi, R. Parvaz, Y. Khedmati Yengejeh, *Three-dimensional and multiple image encryption algorithm using a fractional-order chaotic system*, Computation **13(5)** (2025).

[24] A. Ghoreyshi, M. Abbaszadeh, M.A. Zaky, M. Dehghan, *Finite block method for nonlinear time-fractional partial integro-differential equations: stability, convergence, and numerical analysis*, Appl. Numer. Math. **214** (2025).

[25] A. Ghoreyshi, M. Abbaszadeh, M.A. Zaky, M. Dehghan, *An accurate and robust numerical method for solving distributed-order space–time fractional PDEs*, Z. Angew. Math. Phys. **76(6)** (2025).

[26] A. Ghoreyshi, M. Abbaszadeh, M.A. Zaky, M. Dehghan, *Two high-order numerical schemes based on the Lagrange polynomials for solving a distributed-order time-fractional partial integro-differential equation on non-rectangular domains*, J. Appl. Math. Comput. **71(5)** (2025).

[27] A. Ghoreyshi, M. Zaky, M. Abbaszadeh, M. Dehghan, *An efficient numerical scheme for time-fractional partial integro-differential equations with time delay on rectangular and non-rectangular domains*, Comput. Appl. Math. **45(10)** (2026).

[28] A. Ghoreyshi, M. Abbaszadeh, M. Dehghan, *Numerical methods for the time-fractional diffusion equation: A review*, AUT J. Math. Comput. **7(2)** (2026).

[29] A.A.M. Ghuraibawi, H.R. Marasi, M.H. Derakhshan, P. Kumar, *Numerical solution of multidimensional time-space fractional differential equations of distributed order with Riesz derivative*, Math. Methods Appl. Sci. **46(14)** (2023).

[30] M.H. Heydari, M. Razzaghi, *Orthonormal discrete Legendre polynomials for stochastic distributed-order time-fractional fourth-order delay sub-diffusion equation*, Math. Methods Appl. Sci. **47(18)** (2024).

[31] S. Irandoust-Pakchin, M.H. Derakhshan, *A study on an efficient method based on the mixed finite element scheme for solving a fourth-order time-fractional model involving the Riesz space-fractional derivative of distributed order along with a stability analysis*, J. Appl. Math. Comput. (2025).

[32] J.T. Katsikadelis, *Numerical solution of distributed order fractional differential equations*, J. Comput. Phys. **259** (2014), 11-22.

[33] S. Kosari, P. Xu, J. Shafi, M. Derakhshan, *An efficient hybrid numerical approach for solving two-dimensional fractional cable model involving time-fractional operator of distributed order with error analysis*, Numer. Algorithms (2024).

[34] S. Kosari, M. Derakhshan, *An efficient numerical approach for solving time-space fractional wave model of multiterm order involving the Riesz fractional operators of distributed order with the weakly singular kernel along with stability analysis*, Math. Methods Appl. Sci. **48(9)** (2025).

[35] T. Kosztołowicz, *Subdiffusion equation with fractional Caputo time derivative with respect to another function in modeling transition from ordinary subdiffusion to superdiffusion*, Phys. Rev. E **107(6)** (2023).

[36] Y. Kumar, S. Singh, N. Srivastava, A. Singh, V.K. Singh, *Wavelet approximation scheme for distributed order fractional differential equations*, Comput. Math. Appl. **80(8)** (2020).

[37] X. Li, P.J. Wong, *Two new approximations for generalized Caputo fractional derivative and their application in solving generalized fractional sub-diffusion equations*, J. Appl. Math. Comput. **69(6)** (2023).

[38] M. Li, W. Li, Z. Du, T. Hou, *A maximum bound principle preserving CN/AB finite difference scheme for Riesz space-fractional Allen-Cahn equations with logarithmic free energy*, Adv. Continuous Discrete Models **2025(1)** (2025).

[39] H.L. Liao, N. Liu, X. Zhao, *Asymptotically compatible energy of variable-step fractional BDF2 scheme for the time-fractional Cahn–Hilliard model*, IMA J. Numer. Anal. **45(3)** (2025).

[40] S. Lu, F.J. Molz, H.H. Liu, *An efficient, three-dimensional, anisotropic, fractional Brownian motion and truncated fractional Levy motion simulation algorithm based on successive random additions*, Comput. Geosci. **29(1)** (2003).

[41] Y. Luchko, *Boundary value problems for the generalized time-fractional diffusion equation of distributed order*, Fract. Calc. Appl. Anal. **12(4)** (2009).

[42] F. Mainardi, A. Mura, G. Pagnini, R. Gorenflo, *Time-fractional diffusion of distributed order*, J. Vib. Control **14(9-10)** (2008), 1267-1290.

[43] F. Mainardi, G. Pagnini, R. Gorenflo, *Some aspects of fractional diffusion equations of single and distributed order*, Appl. Math. Comput. **187(1)** (2007), 295-305.

[44] H. Marasi, M. Derakhshan, *A composite collocation method based on the fractional Chelyshkov wavelets for distributed-order fractional mobile-immobile advection-dispersion equation*, Math. Model. Anal. **27(4)** (2022).

[45] H.R. Marasi, M.H. Derakhshan, *Haar wavelet collocation method for variable order fractional integro-differential equations with stability analysis*, Comput. Appl. Math. **41(3)** (2022).

[46] R. Ojha, S. Natesan, *A fourth-order collocation scheme for generalized Black-Scholes model in financial decision-making*, Numer. Algorithms (2025).

[47] M. Pourbabaee, A. Saadatmandi, *A novel Legendre operational matrix for distributed order fractional differential equations*, Appl. Math. Comput. **361** (2019).

[48] M. Pourbabaee, A. Saadatmandi, *The construction of a new operational matrix of the distributed-order fractional derivative using Chebyshev polynomials and its applications*, Int. J. Comput. Math. **98(11)** (2021).

[49] M. Pourbabaee, A. Saadatmandi, *A new operational matrix based on Müntz–Legendre polynomials for solving distributed order fractional differential equations*, Math. Comput. Simulation **194** (2022).

[50] M. Pourbabaee, A. Saadatmandi, *New operational matrix of Riemann–Liouville fractional derivative of orthonormal Bernoulli polynomials for the numerical solution of some distributed-order time-fractional partial differential equations*, J. Appl. Anal. Comput. **13(6)** (2023).

[51] H. Qiao, A. Cheng, *A fast averaged L1 finite difference method for time fractional mobile/immobile diffusion equation with weakly singular solution*, Commun. Appl. Math. Comput. (2025).

[52] P. Rahimkhani, E. Keshavarz Hedayati, R. Moeti, *Solving distributed-order fractional equations via Genocchi wavelets and weighted residual method*, Math. Interdiscip. Res. **11(1)** (2026).

[53] H. Rezaei, M. Asadipour, M.H. Derakhshan, *A stable and convergent fully discrete scheme for solving two-dimensional distributed-order fractional cable models*, J. Math. Model. (2026).

[54] R.K. Saxena, A.M. Mathai, H.J. Haubold, *Distributed order reaction-diffusion systems associated with Caputo derivatives*, J. Math. Phys. **55(8)** (2014).

[55] M. Suliman, M. Ibrahim, E.A. Algehyne, V. Ali, *A study of an efficient numerical method for solving the generalized fractional reaction-diffusion model involving a distributed-order operator along with stability analysis*, Comput. Math. Appl. **180** (2025).

[56] V.E. Tarasov, *Large lattice fractional Fokker–Planck equation*, J. Stat. Mech. Theory Exp. **2014(9)** (2014).

[57] Ž. Tomovski, T. Sandev, *Distributed-order wave equations with composite time fractional derivative*, Int. J. Comput. Math. **95(6-7)** (2018).

[58] J.L. Vázquez, *The Porous Medium Equation: Mathematical Theory*, Oxford University Press, (2007).

[59] F. Wang, Z. Wang, Q. Ma, X. Ding, *A novel explicit fully-discrete momentum-preserving scheme of damped nonlinear stochastic wave equation influenced by multiplicative space-time noise*, Appl. Math. Lett. **160** (2025).

[60] G.C. Wu, D. Baleanu, Z.G. Deng, S.D. Zeng, *Lattice fractional diffusion equation in terms of a Riesz–Caputo difference*, Physica A **438** (2015).

[61] X. Xu, Y. Chen, J. Huang, *L1-type finite element method for time-fractional diffusion-wave equations on nonuniform grid*, Numer. Methods Partial Differential Eq. **40(6)** (2024).

[62] Y.H. Youssri, A.G. Atta, *Explicit Chebyshev collocation method for multi-order fractional nonlinear boundary value problems in mathematical chemistry*, Iranian J. Math. Chem. **16(4)** (2025).

[63] Q. Zhang, T. Gao, T. Chen, Y. Wen, Z. Li, S. Liang, *A wavelet-guided and physics-aware network for remote sensing image dehazing*, Expert Syst. Appl. **285** (2026).

[64] C. Zheng, Z. Du, W. Kang, T. Hou, *Two linearized maximum bound principle preserving finite difference schemes of Riesz space-fractional Allen-Cahn equations with logarithmic free energy*, Int. J. Comput. Math. (2025).

[65] Z.Y. Zheng, Y.M. Wang, *H1-norm analysis of an integral-averaged L1 method on nonuniform time meshes for a time-fractional diffusion problem*, J. Sci. Comput. **103(3)** (2025).

[66] J. Zhou, X. M. Gu, Y. L. Zhao, H. Li, *A fast compact difference scheme with unequal time-steps for the tempered time-fractional Black–Scholes model*, Int. J. Comput. Math. **101(9-10)** (2024).